NR-101 stimulation than after rhTPO stimulation, but their transcriptional levels remained high for long periods. These expression profiles were consistent with the HIF-1α protein levels detected by Western blotting.

Among these HIF-1α–regulated genes, enhanced expression of the *VEGF* gene was confirmed at the protein level by detecting the amount of VEGF secreted into the UT-7/TPO culture supernatant by enzyme-linked immunosorbent assay. NR-101–treated cells produced a higher level of VEGF than did rhTPO-treated cells (Fig. 7D). These results indicated that NR-101 induces a hypoxic response by stabilizing HIF-1α protein more efficiently than TPO does.

## Discussion

In the present study, we identified NR-101 as a novel small-molecule c-MPL agonist, which was originally discovered on screening a chemical library for activity to promote the proliferation of $CD34^+$ cells. NR-101 exhibited an $EC_{50}$ of 0.36 ng/mL in the UT-7/TPO cell proliferation assay, which was comparable to that of rhTPO (0.24 ng/mL), and the maximum activity of NR-101 was also equivalent to that of TPO. It is important to note that NR-101 was superior to another small-molecule c-MPL agonist, SB-497115, in inducing the proliferation of UT-7/TPO cells. NR-101 requires a histidine residue (His499) in the transmembrane domain of c-MPL to exert its activity (data not shown). Many other c-MPL agonists, SB-497115, NIP-004, Butyzamide, and AKR-501, also require this histidine residue in the transmembrane domain of c-MPL [34–39], suggesting that NR-101 selectively binds and activates c-MPL. However, further investigations are needed to clarify the mechanism by which NR-101 activates c-MPL because we have not proved direct binding of NR-101 to c-MPL.

We clearly demonstrated that NR-101 prevails over TPO in the ex vivo expansion of HSCs/HPCs. Although there was no significant difference between rhTPO and NR-101 in expanding total cell numbers and inducing megakaryocytic differentiation from human $CD34^+$ cells, NR-101 preferentially expanded the $CD34^+CD38^-$ population and maintained their colony-forming capacity as compared with rhTPO. This positive effect on $CD34^+CD38^-$ cells is specific to NR-101 because the effect of other nonpeptidyl c-MPL agonists, SB-497115, NIP-004, and AKR-501, on $CD34^+CD38^-$ cells was comparable to that of rhTPO (data not shown), suggesting that the specific structure of NR-101 is responsible for the capacity to expand $CD34^+CD38^-$ cells. Moreover, NR-101 induced a 2.9-fold expansion of SRCs in short-term cultures, whereas rhTPO-treated cultures showed no significant change in SRC numbers compared with fresh $CD34^+$ cells (1.2-fold expansion; $p = 0.51$). The observation that TPO did not expand SRC numbers under serum-free conditions is consistent with recent reports [59–61], suggesting that a combination of the cytokines TPO, SCF, and FL is not sufficient to achieve the expansion of human HSCs in the present culture conditions.

To further understand the effect of NR-101 on HSCs/PCs, we analyzed the cell cycle of the $CD34^+CD38^-$ fraction in cultures with rhTPO or NR-101. NR-101 increased the size of the BrdU-negative fraction ($G_0$ or $G_1$ phase) in $CD34^+CD38^-$ cells more than did rhTPO, while NR-101 had no effect on the cell cycle in $CD34^+CD38^+$ cells or $CD34^+$ cells overall. Intriguingly, NR-101 appeared to increase the proportion of $CD34^+CD38^+$ cells in the $G_1$ phase. These observations indicate that NR-101 promotes the cell cycle arrest of primitive HSCs/HPCs in the $G_1$ phase, but does not induce quiescence ($G_0$ phase) in vitro. This result is consistent with the finding by Danet et al. that hypoxia promotes the transition from $G_0$ to $G_1$ and/or induces cell cycle arrest in $G_1$ in $Lin^-CD34^+$ cells [53]. It has been shown that HSCs remain quiescent or undergo division at a slow rate in BM niches to achieve long-term self-renewal and maintain the capacity to differentiate into multiple lineages. By contrast, in ex vivo cultures, HSCs rapidly cycle and undergo terminal differentiation [62,63]. The NR-101–induced slow cycling of HSCs/PCs might help to protect them from excessive differentiation and allow them to self-renew in culture. However, the expression of negative cell cycle regulators, *p21* and *p27*, in $CD34^+CD38^-$ cells was not significantly affected by NR-101 treatment (data not shown), so the underlying molecular mechanisms remain obscure.

In this study, we noted several unique effects of NR-101 that may explain the molecular mechanisms involved in the expansion of HSCs by NR-101. We found that NR-101 activates c-MPL and its downstream signaling molecules very slowly, but maintains high levels of their activated forms for significantly longer periods as compared to rhTPO. It is conceivable that the resistance of chemical compounds to degradation during culture and/or less internalization of c-MPL into the cytoplasm account for the sustained effects of NR-101. Importantly, NR-101 persistently activates STAT5, but hardly activates STAT3. STAT5 plays an essential role in the self-renewal of HSCs [45]. The specific and durable activation of STAT5 by NR-101 might contribute to the augmented self-renewal capacity of HSCs. On the other hand, this finding also suggests that STAT3 is not absolutely essential to the maintenance of self-renewing HSCs in vitro. Taking into account the occasional uncertainty of results obtained by cell line-based evaluation, additional studies using $CD34^+$ and $CD34^+CD38^-$ cells would be necessary to confirm the characteristic cell signaling by NR-101 and actual roles of STAT proteins.

The hypoxic response mediated by HIF-1α is important for the maintenance of HSCs and hypoxic conditions reportedly enhance the reconstitution activity of HSCs in recipient mice [53,64]. TPO is one of the cytokines that activates hypoxia-responsive pathways by increasing the intranuclear level of HIF-1α [54-56]. NR-101 appeared to efficiently stabilize HIF-1α protein and higher levels of HIF-1α protein

were detected in cells treated with NR-101 than those treated with rhTPO. Consistent with these findings, we found that NR-101 induces the gene expression of targets of HIF-1α more intensively than does TPO. Among the targets of HIF-1α, VEGF has been implicated in the survival of HSCs through an internal autocrine loop [65]. Enhanced glycolysis with reduced mitochondrial respiration is a characteristic metabolic shift observed in embryonic stem cells and hypoxic cancer cells with extensive self-renewal capacity [66,67]. Enhanced expression of *VEGF* and genes involved in glycolysis and glucose transport might favor the maintenance and/or expansion of HSCs/HPCs in NR-101–treated cultures. Thus, the induction of hypoxic responses in HSCs/HPCs could be another mechanism by which NR-101 promotes SRC expansion in vitro. However, further study is needed to clarify the mechanism of stabilization of HIF-1α protein by NR-101 and the involvement of sustained activation of STAT5 in this process.

Numerous investigators have attempted to improve the efficiency of ex vivo expansion of human HSCs for clinical purposes, particularly hCB HSC transplantation. Notably, all recent studies have used TPO and SCF in the cell culture. Therefore, it will be beneficial to substitute NR-101 for TPO in the present culture systems to achieve a more efficient ex vivo expansion of HSCs. The approach using NR-101 has an advantage over other strategies in that NR-101 has the capacity to induce HSC self-renewal and is readily available to combine with other technologies. In addition, NR-101 could be also applied to gene therapy using HSCs, which requires the maintenance of HSCs in the process of gene transduction. It will be important to further attempt to expand HSCs by combining NR-101 with other cytokines, ligands, and chemicals capable of inducing HSC self-renewal (e.g., Delta1, angiopoietin-like 5, IGFBP2, 5-aza-2′-deoxycytidine, diethylaminobenzaldehyde, or FP6) [49,59–61,68]. It will also be important to change the chemical structure of NR-101 to achieve optimum activity for the expansion of HSCs.

In conclusion, we have identified NR-101, a novel nonpeptidyl small-molecule compound, which exhibits a selective and sustained activation of c-MPL. The results reported here demonstrate that NR-101 is sufficient to induce the expansion of human HSCs. The approach using NR-101 will provide a wider range of options and be useful for the development of novel and efficient technologies for stem cell and gene therapies.

## Acknowledgments

We thank Dr. T. Nakamura for providing the Ba/F3 cells expressing mutated c-MPL, I. Ootsuka for technical assistance, Dr. N. Komatsu for UT-7, UT-7/TPO, and UT-7/EPO cells and Tokyo Cord Blood Bank (Katsushika-ku, Tokyo, Japan) for human cord blood. This work was financially supported by Nissan Chemical Industries, Ltd. (Chiyoda-ku, Tokyo, Japan) and ReproCell Inc. (Minato-ku, Tokyo, Japan).

## Conflict of Interest Disclosure

No financial interest/relationships with financial interest relating to the topic of this article have been declared.

## References

1. de Sauvage FJ, Hass PE, Spencer SD, et al. Stimulation of megakaryocytopoiesis and thrombopoiesis by the c-Mpl ligand. Nature. 1994;369:533–538.
2. Lok S, Kaushansky K, Holly RD, et al. Cloning and expression of murine thrombopoietin cDNA and stimulation of platelet production in vivo. Nature. 1994;369:565–568.
3. Kaushansky K, Lok S, Holly RD, et al. Promotion of megakaryocyte progenitor expansion and differentiation by the c-Mpl ligand thrombopoietin. Nature. 1994;369:568–571.
4. Wendling F, Maraskovsky E, Debili N, et al. c-Mpl ligand is a humoral regulator of megakaryocytopoiesis. Nature. 1994;369:571–574.
5. Bartley TD, Bogenberger J, Hunt P, et al. Identification and cloning of a megakaryocyte growth and development factor that is a ligand for the cytokine receptor Mpl. Cell. 1994;77:1117–1124.
6. Sasaki K, Odai H, Hanazono Y, et al. TPO/c-mpl ligand induces tyrosine phosphorylation of multiple cellular proteins including proto-oncogene products, Vav and c-Cbl, and Ras signaling molecules. Biochem Biophys Res Commun. 1995;216:338–347.
7. Drachman JG, Griffin JD, Kaushansky K. The c-Mpl ligand (thrombopoietin) stimulates tyrosine phosphorylation of Jak2, Shc, and c-Mpl. J Biol Chem. 1995;270:4979–4982.
8. Ezumi Y, Takayama H, OkumaThrombopoietin M. c-Mpl ligand, induces tyrosine phosphorylation of Tyk2, JAK2, and STAT3, and enhances agonists-induced aggregation in platelets in vitro. FEBS Lett. 1995;374:48–52.
9. Bacon CM, Tortolani PJ, Shimosaka A, et al. Thrombopoietin (TPO) induces tyrosine phosphorylation and activation of STAT5 and STAT3. FEBS Lett. 1995;370:63–68.
10. Rojnuckarin P, Drachman JG, Kaushansky K. Thrombopoietin-induced activation of the mitogen-activated protein kinase (MAPK) pathway in normal megakaryocytes: role in endomitosis. Blood. 1999;94:1273–1282.
11. Miyakawa Y, Rojnuckarin P, Habib T, Kaushansky K. Thrombopoietin induces phosphoinositol 3-kinase activation through SHP2, Gab, and insulin receptor substrate proteins in BAF3 cells and primary murine megakaryocytes. J Biol Chem. 2001;276:2494–2502.
12. Sattler M, Salgia R, Durstin MA, Prasad KV, Griffin JD. Thrombopoietin induces activation of the phosphatidylinositol-3′ kinase pathway and formation of a complex containing p85PI3K and the protooncoprotein p120CBL. J Cell Physiol. 1997;171:28–33.
13. Solar GP, Kerr WG, Zeigler FC, et al. Role of c-mpl in early hematopoiesis. Blood. 1998;92:4–10.
14. Sitnicka E, Lin N, Priestley GV, et al. The effect of thrombopoietin on the proliferation and differentiation of murine hematopoietic stem cells. Blood. 1996;87:4998–5005.
15. Kaushansky K. Thrombopoietin: accumulating evidence for an important biological effect on the hematopoietic stem cell. Ann N Y Acad Sci. 2003;996:39–43.
16. Buza-Vidas N, Antonchuk J, Qian H, et al. Cytokines regulate postnatal hematopoietic stem cell expansion: opposing roles of thrombopoietin and LNK. Genes Dev. 2006;20:2018–2023.
17. Yoshihara H, Arai F, Hosokawa K, et al. Thrombopoietin/MPL signaling regulates hematopoietic stem cell quiescence and interaction with the osteoblastic niche. Cell Stem Cell. 2007;1:685–697.
18. Qian H, Buza-Vidas N, Hyland CD, et al. Critical role of thrombopoietin in maintaining adult quiescent hematopoietic stem cells. Cell Stem Cell. 2007;1:671–684.

19. Kimura S, Roberts AW, Metcalf D, Alexander WS. Hematopoietic stem cell deficiencies in mice lacking c-Mpl, the receptor for thrombopoietin. Proc Natl Acad Sci U S A. 1998;95:1195–1200.
20. Fox N, Priestley G, Papayannopoulou T, Kaushansky K. Thrombopoietin expands hematopoietic stem cells after transplantation. J Clin Invest. 2002;110:389–394.
21. Seita J, Ema H, Ooehara J, et al. Lnk negatively regulates self-renewal of hematopoietic stem cells by modifying thrombopoietin-mediated signal transduction. Proc Natl Acad Sci U S A. 2007; 104:2349–2354.
22. Ogawa M. Differentiation and proliferation of hematopoietic stem cells. Blood. 1993;81:2844–2853.
23. Kondo M, Wagers AJ, Manz MG, et al. Biology of hematopoietic stem cells and progenitors: implications for clinical application. Annu Rev Immunol. 2003;21:759–806.
24. Shizuru JA, Negrin RS, Weissman IL. Hematopoietic stem and progenitor cells Clinical and preclinical regeneration of the hematolymphoid system. Annu Rev Med. 2005;56:509–538.
25. Verma IM, Weitzman MD. Gene therapy: twenty-first century medicine. Annu Rev Biochem. 2005;74:711–738.
26. Sauvageau G, Iscove NN, Humphries RK. In vitro and in vivo expansion of hematopoietic stem cells. Oncogene. 2004;23:7223–7232.
27. Sorrentino BP. Clinical strategies for expansion of haematopoietic stem cells. Nat Rev Immunol. 2004;4:878–888.
28. Hofmeister CC, Zhang J, Knight KL, Le P, Stiff PJ. Ex vivo expansion of umbilical cord blood stem cells for transplantation: growing knowledge from the hematopoietic niche. Bone Marrow Transplant. 2007; 39:11–23.
29. Piacibello W, Sanavio F, Garetto L, et al. Extensive amplification and self-renewal of human primitive hematopoietic stem cells from cord blood. Blood. 1997;89:2644–2653.
30. Blank U, Karlsson G, Karlsson S. Signaling pathways governing stem-cell fate. Blood. 2008;111:492–503.
31. Oostendorp RA, Audet J, Miller C, Eaves CJ. Cell division tracking and expansion of hematopoietic long-term repopulating cells. Leukemia. 1999;13:499–501.
32. Li J, Yang C, Xia Y, et al. Thrombocytopenia caused by the development of antibodies to thrombopoietin. Blood. 2001;98:3241–3248.
33. Basser RL, O'Flaherty E, Green M, et al. Development of pancytopenia with neutralizing antibodies to thrombopoietin after multicycle chemotherapy supported by megakaryocyte growth and development factor. Blood. 2002;99:2599–2602.
34. Kuter DJ. New thrombopoietic growth factors. Blood. 2007;109:4607–4616.
35. Erickson-Miller CL, Delorme E, Tian SS, et al. Preclinical activity of Eltrombopag (SB-497115), an oral, non-peptidé thrombopoietin receptor agonist. Stem Cells. 2009;27:424–430.
36. Bussel JB, Provan D, Shamsi T, et al. Effect of eltrombopag on platelet counts and bleeding during treatment of chronic idiopathic thrombocytopenic purpura: a randomised, double-blind, placebo-controlled trial. Lancet. 2009;373:641–648.
37. Fukushima-Shintani M, Suzuki K, Iwatsuki Y, et al. AKR-501 (YM477) a novel orally-active thrombopoietin receptor agonist. Eur J Haematol. 2009;82:247–254.
38. Nakamura T, Miyakawa Y, Miyamura A, et al. A novel nonpeptidyl human c-Mpl activator stimulates human megakaryopoiesis and thrombopoiesis. Blood. 2006;107:4300–4307.
39. Nogami W, Yoshida H, Koizumi K, et al. The effect of a novel, small non-peptidyl molecule butyzamide on human thrombopoietin receptor and megakaryopoiesis. Haematologica. 2008;93:1495–1504.
40. Komatsu N, Kunitama M, Yamada M, et al. Establishment and characterization of the thrombopoietin-dependent megakaryocytic cell line, UT-7/TPO. Blood. 1996;87:4552–4460.
41. Komatsu N, Nakauchi H, Miwa A, et al. Establishment and characterization of a human leukemic cell line with megakaryocytic features: dependency on granulocyte-macrophage colony-stimulating factor, interleukin 3, or erythropoietin for growth and survival. Cancer Research. 1991;51:341–348.
42. Komatsu N, Yamamoto M, Fujita H, et al. Establishment and characterization of an erythropoietin-dependent subline, UT-7/Epo, derived from human leukemia cell line, UT-7. Blood. 1993;82: 456–464.
43. Dao MA, Nolta JA. Cytokine and integrin stimulation synergize to promote higher levels of GATA-2, c-myb, and CD34 protein in primary human hematopoietic progenitors from bone marrow. Blood. 2007;109:2373–2379.
44. Francoeur A, Assalian A. Microcat: a novel cell proliferation and cytotoxicity assay based on WST-1. Biochemica. 1996;3:19–25.
45. Kato Y, Iwama A, Tadokoro Y, et al. Selective activation of STAT5 unveils its role in stem cell self-renewal in normal and leukemic hematopoiesis. J Exp Med. 2005;202:169–179.
46. Larochelle A, Vormoor J, Hanenberg H, et al. Identification of primitive human hematopoietic cells capable of repopulating NOD/SCID mouse bone marrow: implications for gene therapy. Nat Med. 1996; 2:1329–1337.
47. Pflumió F, Izac B, Katz A, et al. Phenotype and function of human hematopoietic cells engrafting immune-deficient CB17-severe combined immunodeficiency mice and nonobese diabetic-severe combined immunodeficiency mice after transplantation of human cord blood mononuclear cells. Blood. 1996;88:3731–3740.
48. Bhatia M, Wang JC, Kapp U, Bonnet D, Dick JE. Purification of primitive human hematopoietic cells capable of repopulating immune-deficient mice. Proc Natl Acad Sci U S A. 1997;94:5320–5325.
49. Ueda T, Tsuji K, Yoshino H, et al. Expansion of human NOD/SCID-repopulating cells by stem cell factor, Flk2/Flt3 ligand, thrombopoietin, IL-6, and soluble IL-6 receptor. J Clin Invest. 2000;105: 1013–1021.
50. Vainchenker W, Deschamps JF, Bastin JM, Breton-Gorius TJ, McMichael AJ. Two monoclonal antiplatelet antibodies as markers of human megakaryocyte maturation: immunofluorescent staining and platelet peroxidase detection in megakaryocyte colonies and in in vivo cells from normal and leukemic patients. Blood. 1982;59: 514–521.
51. Ohmizono Y, Sakabe H, Kimura T, et al. Thrombopoietin augments ex vivo expansion of human cord blood-derived hematopoietic progenitors in combination with stem cell factor and flt3 ligand. Leukemia. 1997;11:524–530.
52. McNiece IK, Stewart DM, Deacon DM, et al. Detection of a human CFC with a high proliferative potential. Blood. 1989;74:609–612.
53. Danet GH, Pan Y, Luongo JL, Bonnet DA, Simon MC. Expansion of human SCID-repopulating cells under hypoxic conditions. J Clin Invest. 2003;112:126–135.
54. Kirito K, Fox N, Komatsu N, Kaushansky K. Thrombopoietin enhances expression of vascular endothelial growth factor (VEGF) in primitive hematopoietic cells through induction of HIF-1alpha. Blood. 2005;105:4258–4263.
55. Kirito K, Kaushansky K. Thrombopoietin stimulates vascular endothelial cell growth factor (VEGF) production in hematopoietic stem cells. Cell Cycle. 2005;4:1729–1731.
56. Zhou J, Brüne B. Cytokines and hormones in the regulation of hypoxia inducible factor-1alpha (HIF-1alpha). Cardiovasc Hematol Agents Med Chem. 2006;4:189–197.
57. Wang GL, Semenza GL. General involvement of hypoxia-inducible factor 1 in transcriptional response to hypoxia. Proc Natl Acad Sci U S A. 1993;90:4304–4308.
58. Huang LE, Bunn HF. Hypoxia-inducible factor and its biomedical relevance. J Biol Chem. 2003;278:19575–19578.
59. Suzuki T, Yokoyama Y, Kumano K, et al. Highly efficient ex vivo expansion of human hematopoietic stem cells using Delta1-Fc chimeric protein. Stem Cells. 2006;24:2456–2465.

60. Zhang CC, Kaba M, Iizuka S, Huynh H, Lodish HF. Angiopoietin-like 5 and IGFBP2 stimulate ex vivo expansion of human cord blood hematopoietic stem cells as assayed by NOD/SCID transplantation. Blood. 2008;111:3415–3423.
61. Chute JP, Muramoto GG, Whitesides J, et al. Inhibition of aldehyde dehydrogenase and retinoid signaling induces the expansion of human hematopoietic stem cells. Proc Natl Acad Sci U S A. 2006;103:11707–11712.
62. Wagner W, Ansorge A, Wirkner U, et al. Molecular evidence for stem cell function of the slow-dividing fraction among human hematopoietic progenitor cells by genome-wide analysis. Blood. 2004;104:675–686.
63. Mahmud N, Devine SM, Weller KP, et al. The relative quiescence of hematopoietic stem cells in nonhuman primates. Blood. 2001;97:3061–3068.
64. Shima H, Takubo K, Iwasaki H, et al. Reconstitution activity of hypoxic cultured human cord blood CD34-positive cells in NOG mice. Biochem Biophys Res Commun. 2009;378:467–472.
65. Gerber HP, Malik AK, Solar GP, et al. VEGF regulates haematopoietic stem cell survival by an internal autocrine loop mechanism. Nature. 2002;417:954–958.
66. Kondoh H. Cellular life span and the Warburg effect. Exp Cell Res. 2008;314:1923–1928.
67. Keith B, Simon MC. Hypoxia-inducible factors, stem cells, and cancer. Cell. 2007;129:465–472.
68. Araki H, Mahmud N, Milhem M, et al. Expansion of human umbilical cord blood SCID-repopulating cells using chromatin-modifying agents. Exp Hematol. 2006;34:140–149.

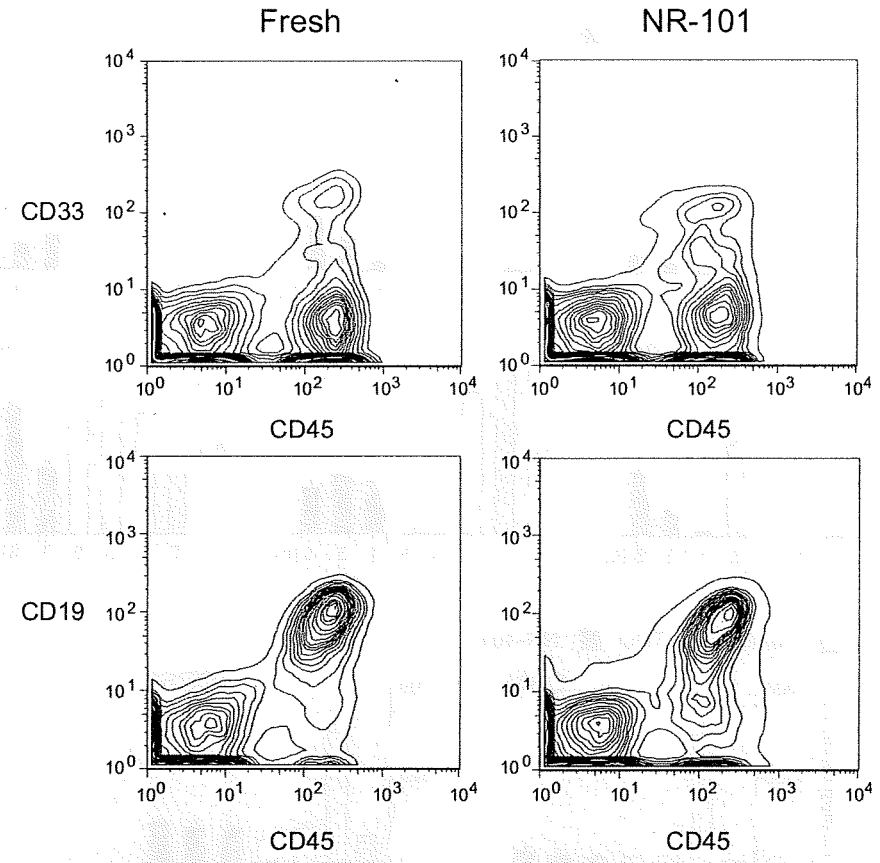


**Supplementary Figure E1.** NR-101-treated cells repopulate both myeloid-lineage and B cell-lineage cells in immunodeficient mice. Representative flow cytometric dot plots showing the repopulation of human $CD33^+$ myeloid-lineage cells and $CD19^+$ B cell-lineage cells by fresh hCB $CD34^+$ cells and NR-101-treated hCB $CD34^+$ cells in NOD/SCID mouse BM 8 weeks after transplantation.

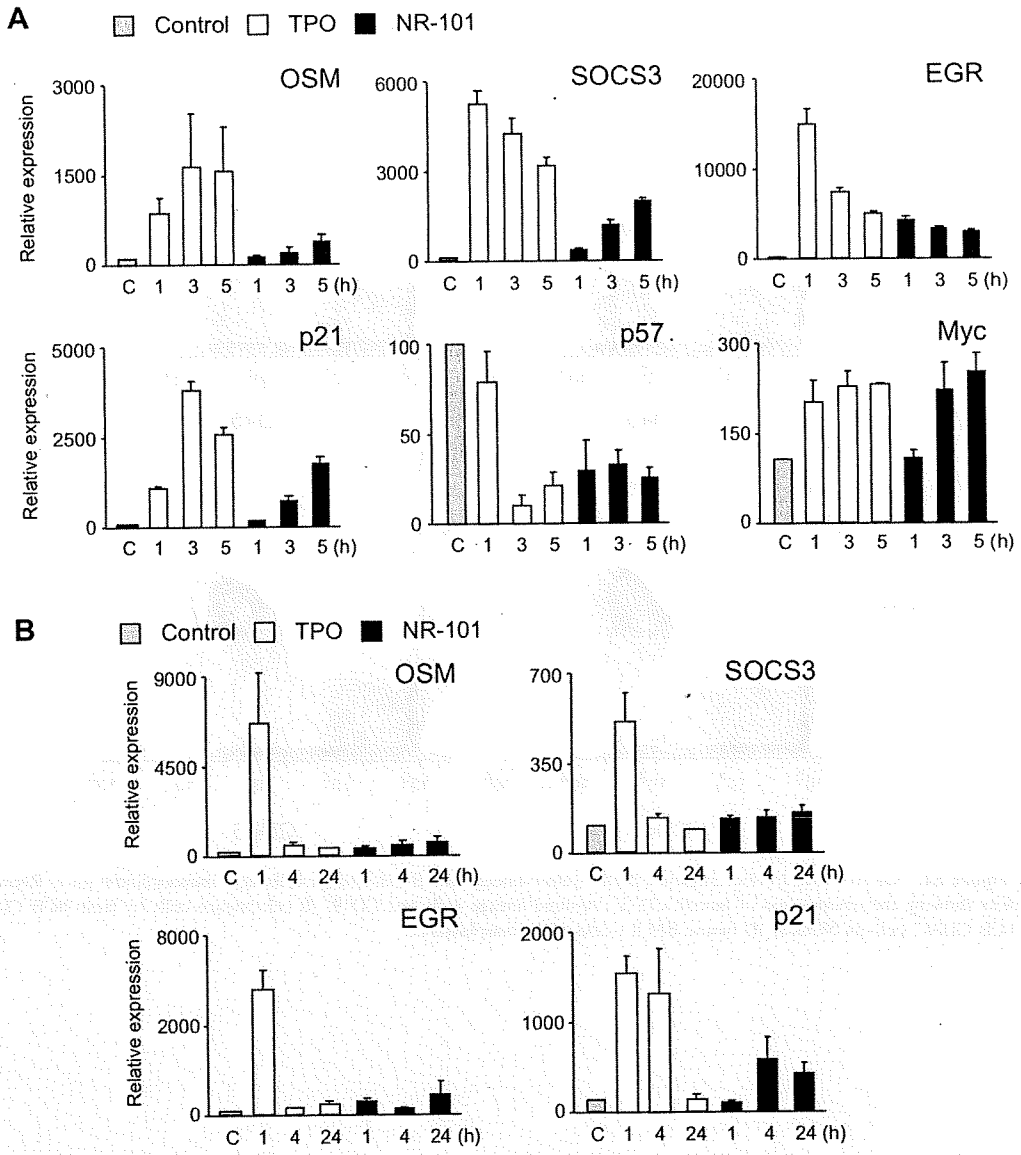


**Supplementary Figure E2.** NR-101 enhances the expression of genes downstream of TPO. UT-7/TPO (**A**) or hCB $CD34^+$ (**B**) cells were stimulated with rhTPO or NR-101 for the period of time indicated. Total RNA was then extracted from cultured cells and the relative expression level of genes (*OSM*, *SOCS3*, *EGR*, *p21*, *p57*, and *c-Myc*) was measured by real-time quantitative PCR. 18S ribosomal RNA (18Sr) or beta-2-microglobulin (B2M) was used as an internal control, and a standard curve was used to quantify mRNA. Bars show mRNA levels in rhTPO or NR-101-stimulated cells at the indicated time points relative to those in DMSO (control: C)-treated cells for 1 hour. Data represent the mean ± SEM (n=3-5).

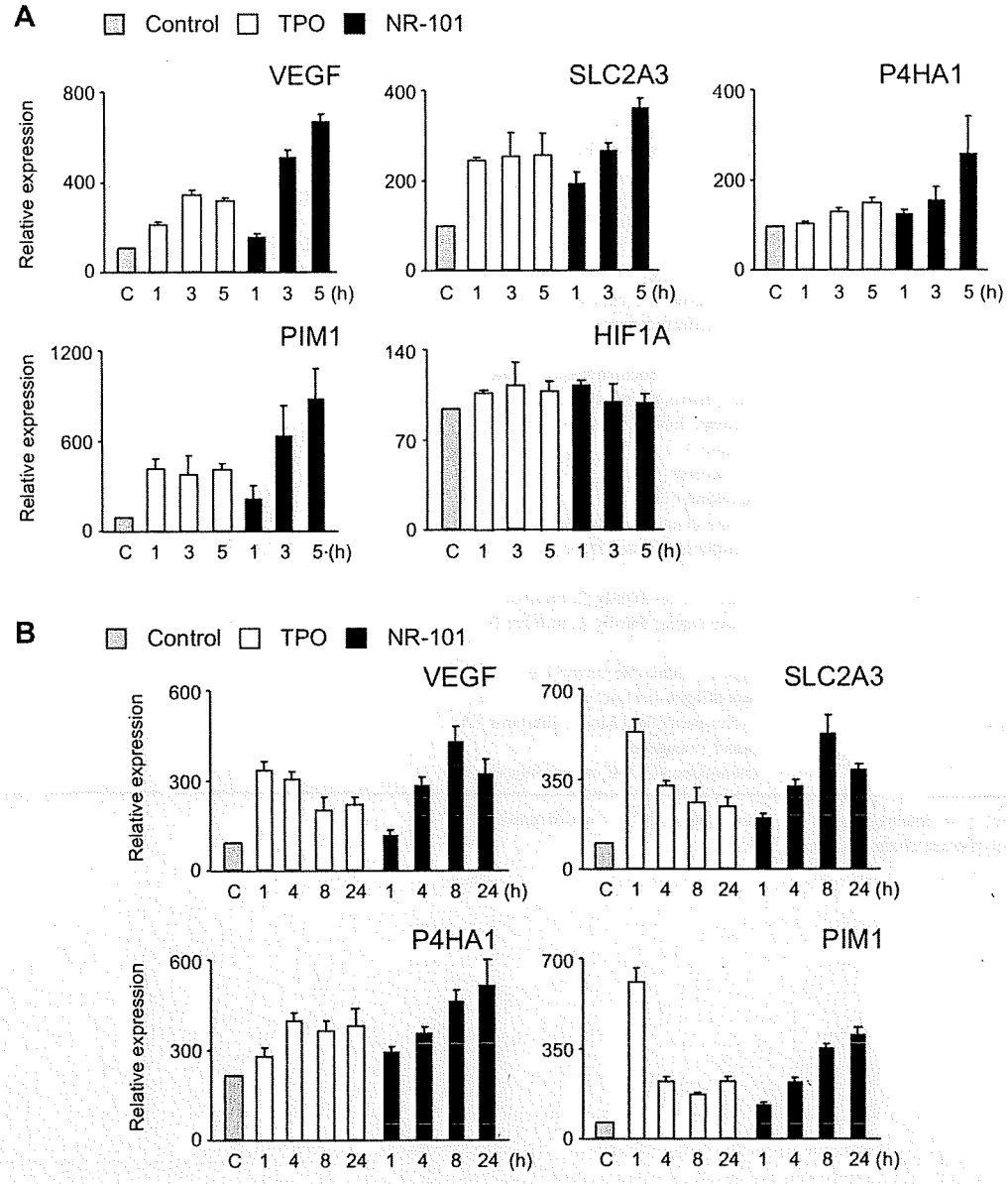


**Supplementary Figure E3.** NR-101 enhances the expression of genes downstream of HIF-1α. UT-7/TPO (**A**) or hCB $CD34^+$ (**B**) cells were stimulated with rhTPO or NR-101 for the period of time indicated. Total RNA was then extracted from cultured cells and the relative expression level of genes (*VEGF*, *SLC2A3*, *P4HA1*, *PIM1*, and *HIF1A*) was measured by real-time quantitative PCR. 18S ribosomal RNA (18Sr) or beta-2-microglobulin (B2M) was used as an internal control, and a standard curve was used to quantify mRNA. Bars show mRNA levels in rhTPO or NR-101-stimulated cells at the indicated time points relative to those in DMSO (control: C)-treated cells for 1 hour. Data represent the mean ± SEM (n=3–5).

**Supplementary Table E1. Expression profiles of hypoxia-inducible factor-1α–inducible genes in cells treated with NR-101[a]**

| Gene symbol | Gene name | UT-7/TPO | $CD34^+$ |
|---|---|---|---|
| Angiogenesis | | | |
| VEGFA | vascular endothelial growth factor A | ↑ | ↑ |
| SERPINE1 | serpin peptidase inhibitor | ↑ | ND |
| Vasomotor control | | | |
| NOS2A | nitric oxide synthase 2A | ↑ | ND |
| EDN1 | endothelin 1 | ↑ | ND |
| Erythropoiesis | | | |
| EPO | erythropoietin | → | ND |
| EPOR | erythropoietin receptor | ↓ | ND |
| TFRC | transferrin receptor | ↑ | ND |
| Glycolysis | | | |
| ALDOA | aldolase A, fructose-bisphosphate | ↑ | ND |
| PFKL | phosphofructokinase, liver | → | ND |
| PKM2 | pyruvate kinase, muscle | → | ND |
| ENO1 | enolase 1 | ↑ | ND |
| HK1 | hexokinase 1 | → | ND |
| HK2 | hexokinase 2 | ↑ | ND |
| LDHA | lactate dehydrogenase A | ↑ | ND |
| PGK1 | phosphoglycerate kinase 1 | → | ND |
| Glucose transport | | | |
| SLC2A1 | solute carrier family 2, number 1 | ↑ | ND |
| SLC2A3 | solute carrier family 2, number 3 | ↑ | ↑ |
| Others | | | |
| HIF1A | hypoxia-inducible factor 1 α | → | ND |
| P4HA1 | procollagen-proline, α 1 | ↑ | ↑ |
| CDKN1A (p21) | cyclin-dependent kinase inhibitor 1A | ↑ | ↑ |
| PIM1 | pim-1 oncogene | ↑ | ↑ |
| CXCL12 | chemokine (C-X-C motif) ligand 12 | ↑ | ↑ |

↑ = upregulated; ↓ = downregulated; → = unchanged; ND = not determined.
[a]Quantitative polymerase chain reaction.

Brief report

# Definitive proof for direct reprogramming of hematopoietic cells to pluripotency

*Motohito Okabe,[1] *Makoto Otsu,[1] Dong Hyuck Ahn,[1] Toshihiro Kobayashi,[1] Yohei Morita,[1] Yukiko Wakiyama,[2] Masafumi Onodera,[3] Koji Eto,[1] Hideo Ema,[1] and Hiromitsu Nakauchi[1,2]

[1]Division of Stem Cell Therapy, Center for Stem Cell and Regenerative Medicine, Institute of Medical Science, University of Tokyo, Tokyo; [2]Japan Science and Technology Agency, Exploratory Research for Advanced Technology, Nakauchi Stem Cell and Organ Regeneration Project, Tokyo; and [3]Department of Genetics, National Research Institute for Child Health and Development, Tokyo, Japan

**Generation of induced pluripotent stem cells (iPSCs) generally uses fibroblastic cells, but other cell sources may prove useful in both research and clinical settings. Although proof of cellular origin requires genetic-marker identification in both target cells and established iPSCs, somatic cells other than mature lymphocytes mostly lack such markers. Here we show definitive proof of direct reprogramming of murine hematopoietic cells with no rearranged genes. Using iPSC factor transduction, we successfully derived iPSCs from bone marrow progenitor cells obtained from a mouse whose hematopoiesis was reconstituted from a single congenic hematopoietic stem cell. Established clones were demonstrated to be genetically identical to the transplanted single hematopoietic stem cell, thus proving their cellular origin. These hematopoietic cell–derived iPSCs showed typical characteristics of iPSCs, including the ability to contribute to chimerism in mice. These results will prompt further use of hematopoietic cells for iPSC generation while enabling definitive studies to test how cellular sources influence characteristics of descendant iPSCs. (Blood. 2009; 114:1764-1767)**

## Introduction

Development of induced pluripotent stem cell (iPSC) technology has enabled generation of disease-specific pluripotent stem cells from the patient.[1] A typical method uses virus-mediated transfer of defined factors into fibroblastic cells[2-4] or marrow-derived mesenchymal cells.[1,5] Some other tissues are also reported as sources for iPSC generation, including murine hepatocytes and gastric epithelial cells,[6] human keratinocytes,[7] and very recently, human blood.[8] As the variability of cellular sources becomes greater, it is attractive to address an interesting question: is each iPSC clone derived from distinct sources unique in its characteristics? Although definitive proof of iPSC cellular origin requires genetic markers, as most somatic cells (except mature lymphocytes) lack such markers, no formal data have shown reprogramming of hematopoietic cells, aside from one study that used immunoglobulin genes as markers.[9] Here, we demonstrate definitive proof for a direct reprogramming to pluripotency of primary marrow hematopoietic cells with no gene rearrangement.

## Methods

### Mice

Animal experiments were performed with approval of the Institutional Animal Care and Use Committee of the Institute of Medical Science, University of Tokyo.

### Generation of iPSCs from murine bone marrow progenitor cells

Lineage marker–negative ($Lin^-$) c-$Kit^+$ ($Kit^+$) cells were enriched using immunomagnetic beads. pMXs vectors[10] encoding iPSC genes are described.[1] Concentrated vesicular stomatitis virus-G–retroviral supernatant was prepared using reported procedures.[11-13] 293GP and 293GPG cells were kind gifts from Dr R. C. Mulligan (Children's Hospital Boston, Harvard Medical School, Boston, MA).[14] Detailed procedures are described in the text and supplemental data (available on the *Blood* website: see the Supplemental Materials link at the top of the online article).

### In vitro and in vivo assessment of iPSCs

Characteristics of iPSCs were assessed following reported procedures.[1] Primer sequences are shown in supplemental Table 1. Immunoglobulin heavy chain gene rearrangement was analyzed following described methods.[15,16] A single-base difference within *Cd45* exon 25 was analyzed as reported.[17]

## Results and discussion

To prove the cellular origin of iPSC clones formally, use of definitive genetic markers is necessary, as with reported reprogramming of mature B cells[9] and pancreatic beta cells.[18] Even if iPSCs are generated from hematopoietic stem/progenitor cells (HSPCs), nearly 100% positive for the hematopoietic marker CD45, one might argue, in light of reported generation of iPSCs from marrow stromal cells,[1,5] that a small number of nonhematopoietic cells had been reprogrammed. However, no such suitable marker exists for hematopoietic cells (excepting rearranged immunoreceptor genes in mature lymphocytes). We therefore exploited a prominent characteristic of the hematopoietic system: transplantation of a single hematopoietic stem cell (HSC) can reconstitute host hematopoiesis.[19]

Submitted February 4, 2009; accepted May 11, 2009. Prepublished online as *Blood* First Edition paper, June 29, 2009; DOI 10.1182/blood-2009-02-203695.

*M. Okabe and M. Otsu contributed equally to this work.

The online version of this article contains a data supplement.

The publication costs of this article were defrayed in part by page charge payment. Therefore, and solely to indicate this fact, this article is hereby marked "advertisement" in accordance with 18 USC section 1734.

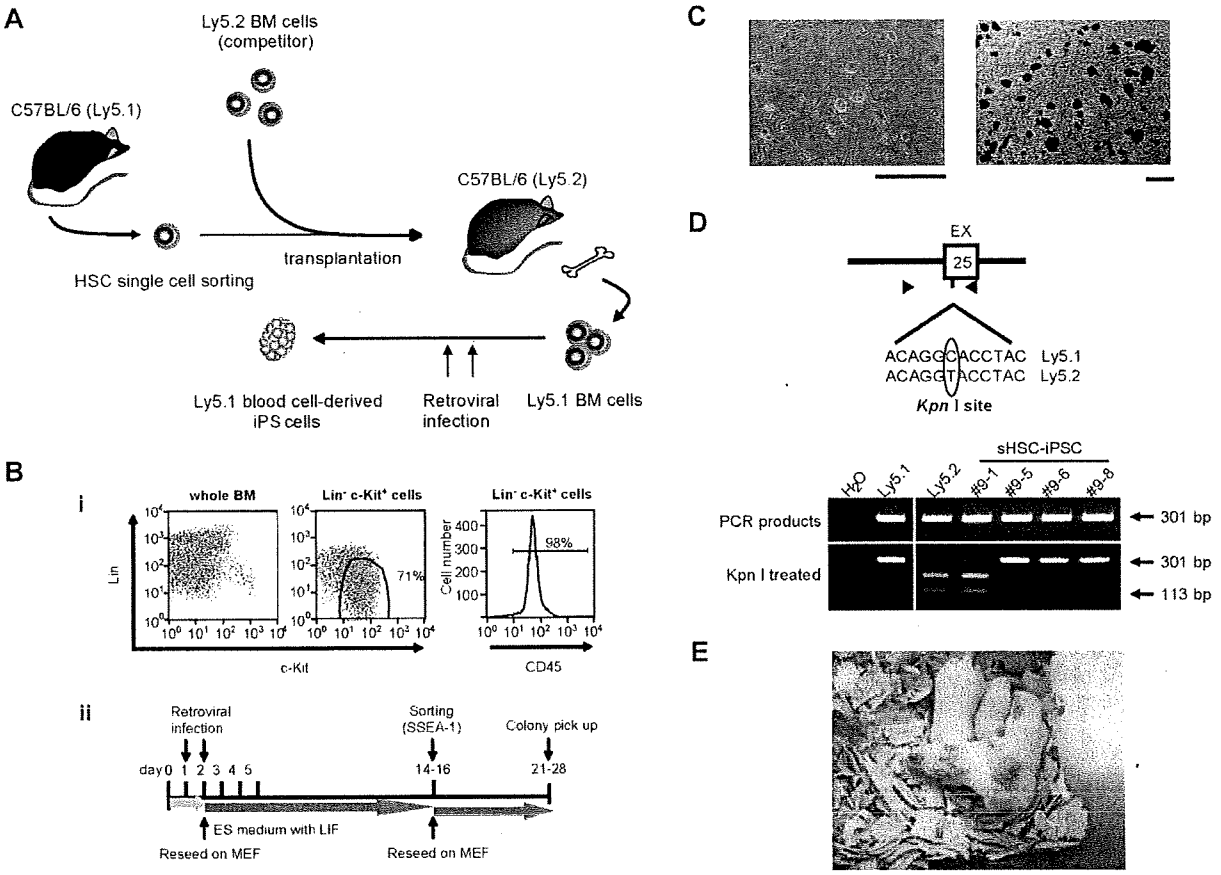


**Figure 1. Proof of iPSC induction from hematopoietic cells in a single-HSC transplantation model.** (A) Schematic representation of the experimental procedure. Single CD150$^+$CD34$^{-/low}$ KSL cells obtained from B6 Ly5.1 mice were transplanted into lethally irradiated B6 Ly5.2 mice together with BM cells from B6 Ly5.2 mice. BM HSPCs were obtained from a recipient mouse that showed long-term (~ 10 months) stable Ly5.1 chimerism (~ 80%), enriched for Ly5.1$^+$ cells, and subjected to iPSC generation. (B) A schematic diagram of iPSC generation from BM HSPCs. (i) Lineage markers (Lin) versus c-Kit plots are shown for cells either before (whole BM) or after (Lin$^-$c-Kit$^+$) purification. Note that purified HSPCs are 98% CD45-positive. (ii) A schematic diagram of iPSC generation from BM HSPCs. (C) Typical ES cell–like appearance of sHSC-iPS cell colonies (left) with high ALP activities (right). Bars represent 100 μm. (D) Determination of the cellular origin of sHSC-iPSC clones. (Top panel) Scheme of the polymerase chain reaction (PCR)–based method used, using a single-base polymorphism at *Cd45* exon (EX) 25. Black triangles represent primer positions. Ly5.1 and Ly5.2 strains differ by a single base in EX 25, as shown in the presented 12-bp sequences from within the 301-bp amplicons. Treatment with the restriction enzyme *Kpn*I leaves the Ly5.1$^+$ cell–derived amplicon undigested, whereas it generates 2 smaller fragments (113 bp + 188 bp) from the Ly5.2$^+$ counterpart. The gel images (bottom panel) indicate that, of 4 sHSC-iPSC clones, 1 (no. 9-1) is of Ly5.2$^+$ cell origin, whereas 3 (nos. 9-5, -6, and -8) are derived from Ly5.1$^+$ cells that originated from a single Ly5.1$^+$ HSC. A vertical line has been inserted to indicate a repositioned gel lane. (E) Chimeric mice obtained by implantation of sHSC-iPSC clone 9-5 into ICR host blastocysts.

Figure 1A depicts our experimental design. We attempted iPSC generation from marrow HSPCs harvested long-term (~ 10 months) after reconstitution from a single HSC of C57BL6 (B6) Ly 5.1 origin. We used concentrated vesicular stomatitis virus-G–pseudotyped retroviruses,[14] as we had succeeded in their efficient transduction into murine HSPCs.[12,13] We purified from bone marrow (BM) of a reconstituted mouse (B6 Ly5.2) Lin$^-$Kit$^+$ cells, a HSPC population, with approximately 98% of cells expressing CD45 (Figure 1B). We then transduced these cells with a cocktail of retroviral vectors harboring each of the iPSC factor genes *Oct4*, *Sox2*, *Klf4*, and *c-Myc*, transferred onto mouse embryonic fibroblast cells, and maintained in the presence of leukemia inhibitory factor until cell sorting (Figure 1B). Visible iPSC-like colonies appeared on approximately days 9 to 11 among a majority of hematopoietic cells that remained nonreprogrammed; these colonies then grew steadily (supplemental Figure 1A). To enrich iPSC candidates, we sorted the cells expressing SSEA-1 on approximately days 14 to 16 and allowed them to regrow for another 7 to 12 days (Figure 1B). Generated iPSC-like colonies showing typical embryonic stem (ES) cell–like appearance were picked up on approximately days 21 to 28. These cells showed robust stability in phenotype, had high alkaline phosphatase (ALP) activity (Figure 1C), and expressed SSEA-1 at levels comparable with those in ES cells (supplemental Figure 1B). In the absence of leukemia inhibitory factor, they readily formed embryoid bodies (data not shown). By using a single-base polymorphism in *CD45*,[17] we could demonstrate that, of the iPSC clones thus established, 3 were derived from Ly5.1$^+$ cells and 1 from a Ly5.2$^+$ cell (Figure 1D). These results formally demonstrate that direct reprogramming of marrow hematopoietic cells is feasible given that transdifferentiation of HSCs to nonhematopoietic lineage cells is, if it ever occurs, an extremely rare event.[20] We named these iPSCs sHSC-iPS cells (sHSC-iPSCs) specifically, when established from BM HSPCs reconstituted from a single HSC.

Each sHSC-iPSC clone was demonstrated to retain proviral sequences of the 4 iPSC factors (supplemental Figure 2A), without detectable transgene expression, probably resulting from gene silencing (supplemental Figure 2B). In contrast, all sHSC-iPSCs were found to express each iPSC factor gene endogenously (supplemental Figure 2B). All sHSC-iPSCs were shown to express the ES cell marker genes *Nanog*, *ERas*, *Rex1*, and *Gdf3* (supplemental Figure 3A). Nanog expression was also confirmed by immunostaining (supplemental Figure 3B). Despite the low expression levels of *Ecat1* and *Zfp296*, another set of ES cell marker genes, these sHSC-iPSCs were shown to

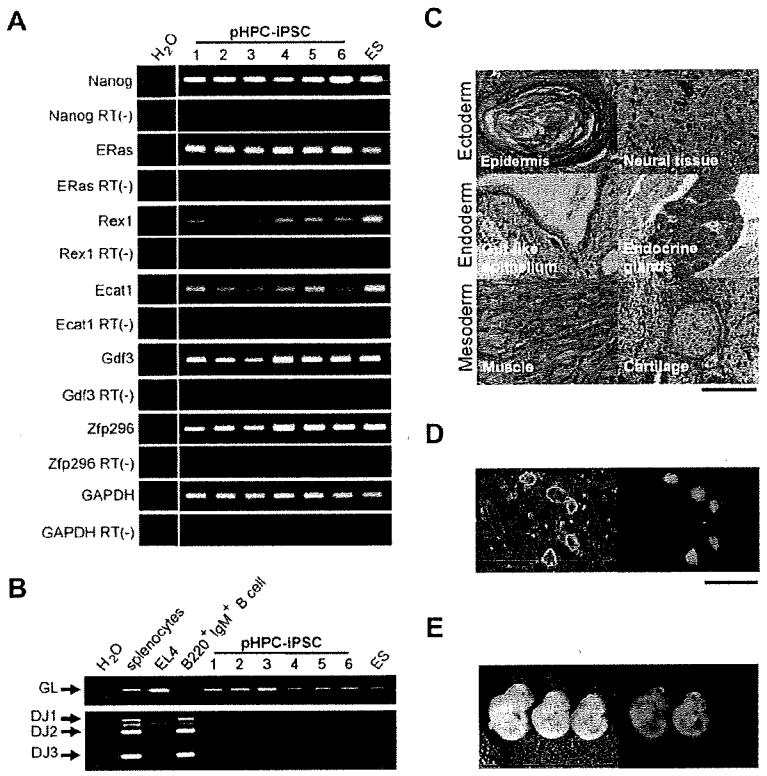


**Figure 2. Characterization of primary BM hematopoietic cell–derived iPSCs generated using the 4 iPSC factors.** (A) Reverse-transcription PCR analysis showing ES marker gene expression in primary BM HSPC-derived iPSC clones (pHPC-iPSCs). $H_2O$ indicates no-template control; ES, ES cells as a positive control; RT (−), no-reverse-transcriptase control. A vertical line has been inserted to indicate a repositioned gel lane. (B) PCR analysis for Ig gene rearrangement of D-J segments (DJ1-DJ3) in pHPC-iPSC clones. GL indicates amplification of the fragment representing unrearranged, germline configuration of the Ig heavy chain gene; EL4, a T lymphoma cell line as an unrearranged control. (C) Histologic sections of teratomas derived from a pHPC-iPSC clone. (D) Images of pHPC-iPSC colonies derived from an EGFP-transgenic mouse. Bars represent 100 μm (C-D). (E) E10.5 chimeric embryos generated with one representative EGFP$^+$ iPSC clone.

be competent in both teratoma formation (supplemental Figure 4) and contribution to chimeric mice (Figure 1E).

We next sought to confirm the reproducibility of direct reprogramming of primary BM HSPCs. Lin$^-$Kit$^+$ BM cells obtained from adult B6 mice were subjected to retrovirus-mediated reprogramming procedures (Figure 1B). From approximately $5 \times 10^5$ HSPCs, we consistently obtained approximately 10 to 30 discrete colonies with typical ES cell–like appearances that stained for ALP (data not shown). Interestingly, iPSC clones established from primary BM HSPCs (pHPC-iPSCs) were shown to express ES cell marker genes more robustly than did sHSC-iPSCs (Figures 2A, S3A). Expression levels in endogenous iPSC factor genes were also more intense in pHPC-iPSCs (supplemental Figure 5B) than in sHSC-iPSCs (supplemental Figure 2B). This may support the idea that huge replicative stress imposed on a single HSC by hematopoietic reconstitution might restrict effective reprogramming of target cells, which are thought to be in senescent states. Confirmation of germline configuration in the immunoglobulin gene revealed the non–B-cell origin of pHPC-iPSCs (Figure 2B). pHPC-iPSCs had the potential for multilineage differentiation, as evidenced by the formation of teratomas, which contained various tissues representing all 3 germ layers (Figure 2C). We were also successful in generating pHPC-iPSCs that constitutively expressed green fluorescence protein from enhanced green fluorescent protein (EGFP)–transgenic mice[21] (Figure 2D). These iPSCs showed a high contribution to embryonic development when microinjected into blastocysts (Figure 2E).

Here we report generation of iPSCs from hematopoietic cells with unrearranged immunoreceptor genes by direct viral transfer of iPSC factors. The principle shown here ensures the feasibility of direct reprogramming of human hematopoietic cells, in conjunction with the recent report of iPSC generation from human blood.[8] The defined cellular origin of our iPSCs enables formal comparative studies using iPSC clones from various sources: One intriguing question is whether or not our iPSC clones differ from those generated from other tissues in respect to reprogramming efficiency, genomic stability, ability of tissue differentiation, and susceptibility to tumorigenesis. Another question is what types of cells in murine HSPCs are actually reprogrammed into iPSCs. At present, we have not yet succeeded in iPSC generation from highly purified HSCs. Considering the germline configuration of the immunoglobulin gene in our iPSC clones (Figure 2B) and the fact that the transduced cells rapidly acquired granulocytic/myeloid-lineage marker expression in our culture conditions (data not shown), myeloid progenitors are currently the plausible target cells of iPSC induction in our system. Studies to address all these issues are ongoing.

## Acknowledgments

The authors thank S. Yamanaka and K. Takahashi for plasmids, R. C. Mulligan for 293GP and 293GPG cells, and H. Kawamoto and T. Ikawa for help with Ig gene analysis.

This work was supported in part by a grant from the Project for Realization of Regenerative Medicine from the Ministry of Education, Culture, Sports, Science and Technology Japan (H.N.) and by the Global Center of Excellence program from the Ministry of Education, Culture, Sports, Science and Technology Japan.

## Authorship

Contribution: M. Okabe generated and characterized iPS cells; M. Otsu generated iPS cells and wrote the manuscript; D.H.A. prepared virus-producing cells; T.K. and Y.W. performed blastocyst injection; Y.M. prepared a single HSC-transplanted chimeric mouse; M. Onodera established transduction procedures

using 293GPG cells; K.E. and H.E. supported experiments with their professional knowledge and experience; and M. Otsu and H.N. supervised the study.

Conflict-of-interest disclosure: The authors declare no competing financial interests.

Correspondence: Hiromitsu Nakauchi, Division of Stem Cell Therapy, Center for Stem Cell and Regenerative Medicine, Institute of Medical Science, University of Tokyo, 4-6-1 Shirokanedai Minato-ku, 108-8639 Tokyo, Japan; e-mail: nakauchi@ims.u-tokyo.ac.jp.

## References

1. Takahashi K, Yamanaka S. Induction of pluripotent stem cells from mouse embryonic and adult fibroblast cultures by defined factors. *Cell.* 2006; 126:663-676.
2. Wernig M, Meissner A, Foreman R, et al. In vitro reprogramming of fibroblasts into a pluripotent ES-cell-like state. *Nature.* 2007;448:318-324.
3. Takahashi K, Okita K, Nakagawa M, Yamanaka S. Induction of pluripotent stem cells from fibroblast cultures. *Nat Protoc.* 2007;2:3081-3089.
4. Yu J, Vodyanik MA, Smuga-Otto K, et al. Induced pluripotent stem cell lines derived from human somatic cells. *Science.* 2007;318:1917-1920.
5. Park IH, Arora N, Huo H, et al. Disease-specific induced pluripotent stem cells. *Cell.* 2008;134: 877-886.
6. Aoi T, Yae K, Nakagawa M, et al. Generation of pluripotent stem cells from adult mouse liver and stomach cells. *Science.* 2008;321:699-702.
7. Aasen T, Raya A, Barrero MJ, et al. Efficient and rapid generation of induced pluripotent stem cells from human keratinocytes. *Nat Biotechnol.* 2008; 26:1276-1284.
8. Loh YH, Agarwal S, Park IH, et al. Generation of induced pluripotent stem cells from human blood. *Blood.* 2009;113:5476-5479.
9. Hanna J, Markoulaki S, Schorderet P, et al. Direct reprogramming of terminally differentiated mature B lymphocytes to pluripotency. *Cell.* 2008;133: 250-264.
10. Onishi M, Kinoshita S, Morikawa Y, et al. Applications of retrovirus-mediated expression cloning. *Exp Hematol.* 1996;24:324-329.
11. Hamanaka S, Nabekura T, Otsu M, et al. Stable transgene expression in mice generated from retrovirally transduced embryonic stem cells. *Mol Ther.* 2007;15:560-565.
12. Nabekura T, Otsu M, Nagasawa T, Nakauchi H, Onodera M. Potent vaccine therapy with dendritic cells genetically modified by the gene-silencing-resistant retroviral vector GCDNsap. *Mol Ther.* 2006;13:301-309.
13. Sanuki S, Hamanaka S, Kaneko S, et al. A new red fluorescent protein that allows efficient marking of murine hematopoietic stem cells. *J Gene Med.* 2008;10:965-971.
14. Ory DS, Neugeboren BA, Mulligan RC. A stable human-derived packaging cell line for production of high titer retrovirus/vesicular stomatitis virus G pseudotypes. *Proc Natl Acad Sci U S A.* 1996;93: 11400-11406.
15. Kawamoto H, Ikawa T, Ohmura K, Fujimoto S, Katsura Y. T cell progenitors emerge earlier than B cell progenitors in the murine fetal liver. *Immunity.* 2000;12:441-450.
16. Schlissel MS, Corcoran LM, Baltimore D. Virus-transformed pre-B cells show ordered activation but not inactivation of immunoglobulin gene rearrangement and transcription. *J Exp Med.* 1991; 173:711-720.
17. Ramos CA, Zheng Y, Colombowala I, Goodell MA. Tracing the origin of non-hematopoietic cells using CD45 PCR restriction fragment length polymorphisms. *Biotechniques.* 2003;34:160-162.
18. Stadtfeld M, Brennand K, Hochedlinger K. Reprogramming of pancreatic beta cells into induced pluripotent stem cells. *Curr Biol.* 2008;18:890-894.
19. Osawa M, Hanada K, Hamada H, Nakauchi H. Long-term lymphohematopoietic reconstitution by a single CD34-low/negative hematopoietic stem cell. *Science.* 1996;273:242-245.
20. Wagers AJ, Sherwood RI, Christensen JL, Weissman IL. Little evidence for developmental plasticity of adult hematopoietic stem cells. *Science.* 2002;297:2256-2259.
21. Okabe M, Ikawa M, Kominami K, Nakanishi T, Nishimune Y. "Green mice" as a source of ubiquitous green cells. *FEBS Lett.* 1997;407:313-319.

OPEN ACCESS Freely available online

PLoS one

# Stepwise Development of Hematopoietic Stem Cells from Embryonic Stem Cells

**Kenji Matsumoto[1], Takayuki Isagawa[2], Toshinobu Nishimura[1], Takunori Ogaeri[1], Koji Eto[1], Satsuki Miyazaki[3], Jun-ichi Miyazaki[3], Hiroyuki Aburatani[2], Hiromitsu Nakauchi[1]*, Hideo Ema[1]***

**1** Division of Stem Cell Therapy, Center for Stem Cell and Regenerative Medicine, Institute of Medical Science, University of Tokyo, Tokyo, Japan, **2** Genome Science Division, Research Center for Advanced Science and Technology, University of Tokyo, Tokyo, Japan, **3** Division of Stem Cell Regulation Research, Osaka University Graduate School of Medicine, Osaka, Japan

## Abstract

The cellular ontogeny of hematopoietic stem cells (HSCs) remains poorly understood because their isolation from and their identification in early developing small embryos are difficult. We attempted to dissect early developmental stages of HSCs using an *in vitro* mouse embryonic stem cell (ESC) differentiation system combined with inducible HOXB4 expression. Here we report the identification of pre-HSCs and an embryonic type of HSCs (embryonic HSCs) as intermediate cells between ESCs and HSCs. Both pre-HSCs and embryonic HSCs were isolated by their c-Kit$^+$CD41$^+$CD45$^-$ phenotype. Pre-HSCs did not engraft in irradiated adult mice. After co-culture with OP9 stromal cells and conditional expression of HOXB4, pre-HSCs gave rise to embryonic HSCs capable of engraftment and long-term reconstitution in irradiated adult mice. Blast colony assays revealed that most hemangioblast activity was detected apart from the pre-HSC population, implying the early divergence of pre-HSCs from hemangioblasts. Gene expression profiling suggests that a particular set of transcripts closely associated with adult HSCs is involved in the transition of pre-HSC to embryonic HSCs. We propose an HSC developmental model in which pre-HSCs and embryonic HSCs sequentially give rise to adult types of HSCs in a stepwise manner.

**Citation:** Matsumoto K, Isagawa T, Nishimura T, Ogaeri T, Eto K, et al. (2009) Stepwise Development of Hematopoietic Stem Cells from Embryonic Stem Cells. PLoS ONE 4(3): e4820. doi:10.1371/journal.pone.0004820

**Editor:** Catherine M. Verfaillie, KU Leuven, Belgium

**Received** November 5, 2008; **Accepted** January 31, 2009; **Published** March 16, 2009



**Funding:** This work was supported by grants from the Ministry of Education, Culture, Sport, Science, and Technology, Japan. These grants have no financial interests, and played no role in study and preparation of the manuscript.

**Competing Interests:** The authors have declared that no competing interests exist.

* E-mail: nakauchi@ims.u-tokyo.ac.jp (HN); hema@ims.u-tokyo.ac.jp (HE)

## Introduction

Mammalian hematopoiesis develops in three distinct waves consisting of primitive hematopoiesis, definitive but transient hematopoiesis, and definitive and persistent hematopoiesis which is established by hematopoietic stem cells (HSCs) [1,2]. Both the first and second hematopoietic waves originate from the yolk sac where hemangioblasts, common precursors of the hematopoietic and endothelial lineages likely play a crucial role [3]. However, whether HSCs arise in either the yolk sac or the paraaortic splanchnopleure/aorta-gonad-mesonephros (P-Sp/AGM) region remains controversial [4,5,6]. The relationship between HSCs and hemangioblasts is also obscure [2,7]. In order to understand how HSCs develop in early embryos, it is important to determine the cellular origin of HSCs rather than the organ origin of HSCs.

Hematopoiesis and vasculogenesis in the early mouse embryo have been recapitulated well by *in vitro* ES differentiation systems [8,9,10]. However, generation of HSCs in substantial numbers from ESCs *in vitro* has been difficult. Kyba *et al.* were the first to report that HSCs can be efficiently generated from ESCs in the OP9 co-culture system by combining this with an inducible HOXB4 expression system (OP9 and iHOXB4 system) [11].

In concept, mesodermal cells first commit to the hematopoietic lineage before giving rise to HSCs. We provisionally called such cells pre-HSCs, and attempted to identify them in embryoid bodies (EB) using the OP9 and iHOXB4 system. We detected the potential to give rise to HSCs among c-Kit$^+$CD41$^+$CD45$^-$ cells derived from ESCs on day 6 of culture (EB6). The presence of hematopoietic progenitor activity in this population has been described [12,13,14]. The present report, however, is the first to document the presence of pre-stem cell activity but little hemangioblast activity in the c-Kit$^+$CD41$^+$CD45$^-$ cell population.

Pre-HSCs gave to an embryonic type of HSCs (embryonic HSCs) capable of reconstituting adult hematopoietic system but at a low degree. OP9 cells supported the transition of pre-HSCs to embryonic HSCs. Some genes were up- and down-regulated during the transition via enforced expression of HOXB4. Interestingly, about two-thirds of the markedly up-regulated genes were also found in our adult HSCs gene expression data. These results suggest that adult HSC-related molecules establish the very early stages of HSC development. Based on these results, we propose an HSC development model in which pre-HSCs through the stage of embryonic HSCs give rise to adult types of HSCs.

## Results

### Experimental design

Our basic experimental strategy consisted of EB formation, co-culture with OP9 cells, and functional assays (Fig. 1). iHOXB4 ESCs were allowed to differentiate spontaneously into EBs for 6 days without HOXB4 expression. We decided to fractionate EB6 cells mainly because by day 6 of culture the number of multipotent

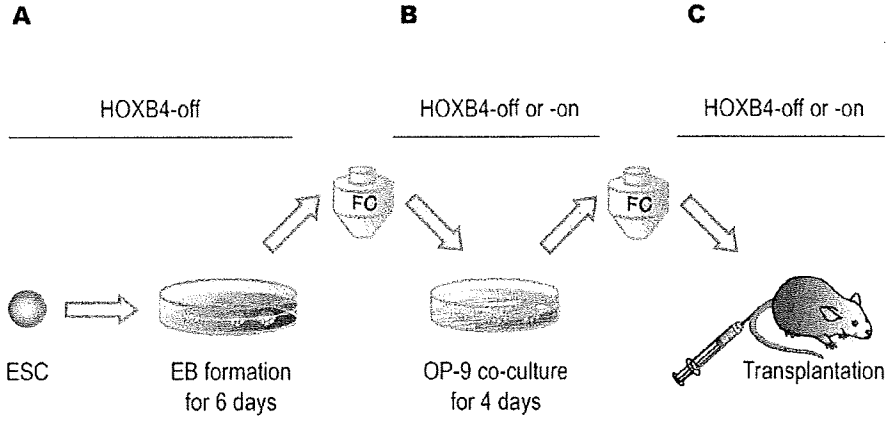


**Figure 1. Study design.** (A) iHOXB4 ESCs were differentiated into EBs for 6 days in the presence of Dox. (B) Dissociated EB cells were analyzed and sorted by flow cytometry (FC). EB cells or their subpopulations were co-cultured with OP9 cells for 4 days in the presence or absence of Dox. (C) Co-cultured cells were analyzed and GFP$^+$ cells were sorted by FC when HOXB4 expression was turned on. Regardless of HOXB4 status in co-cultures, FC sorting was performed on co-cultured cells based on forward and side scatters and on surface markers. Sorted cells were subjected to long-term reconstitution assays. The sorting process turned out to be useful for cell counts, removal of dead cells, and elimination of the remaining Dox.
doi:10.1371/journal.pone.0004820.g001

progenitors reaches a plateau and several surface markers become detectable (Fig. S1). CD41 is known as a marker for the initiation of definitive hematopoiesis [15,16,17,18,19]. As shown in Fig. S1, CD41 appeared in a significant proportion of EB cells on day 6 of culture. Induced HOXB4 expression during EB formation did not affect the generation of colony forming cells and repopulating cells in the OP9 and iHOXB4 system or the appearance of surface markers in EB cells. EB6 cells were analyzed and sorted by flow cytometry. Sorted EB6 cells were co-cultured with OP9 cells for various days under HOXB4-on or -off conditions. The minimal requirement of the co-culture period appeared to be only 4 days (data not shown), which is much shorter than previously thought [11]. After a second analysis and fractionation by flow cytometry, cells were subjected to *in vivo* repopulating assays under HOXB4-on or -off conditions.

## The potential to give rise to HSCs in EB6 subpopulations

EB6 cells were stained with anti-CD41 antibody in combination with anti-CD45, -c-Kit, and -CD34 antibodies and others, and analyzed by flow cytometry (Fig. 2A). CD41$^+$ and CD41$^-$ cells, c-Kit$^+$CD41$^+$ and c-Kit$^-$CD41$^+$ cells, or CD34$^+$CD41$^+$ and CD34$^-$CD41$^+$ cells were sorted by flow cytometry. Sorted cells were co-cultured with OP9 cells for 4 days, and then transplanted into lethally irradiated mice along with rescue cells (Table S1) while HOXB4 expression was maintained from *in vitro* co-culture through *in vivo* repopulation.

Analysis of peripheral blood cells of the recipient mice 16 weeks after transplantation showed that c-Kit$^+$CD41$^+$ cells were enriched in cells with long-term repopulating activity (Fig. 2B). Long-term repopulating activity was similarly detected in both CD34$^-$ and CD34$^+$ cells. Lineage analysis of reconstituted mice showed that myeloid lineage reconstitution predominated. A very low level of B- and T-lymphoid lineage reconstitution was observed only in limited cases. As previously suggested, this might be due to an adverse effect of HOXB4 overexpression [11]. For long-term repopulation, HOXB4 needed to be expressed during the OP9 co-culture period and throughout the repopulation period (data not shown). All these data clearly show that c-Kit$^+$CD41$^+$ cells are the cells that require HOXB4 expression to manifest long-term repopulating activity. In addition, it should be emphasized that CD45 is not expressed in these cells (Fig. 2A).

## Hemangioblasts in EB6 subpopulations

To examine whether c-Kit$^+$CD41$^+$ cells have hemangioblastic activity, we performed blast colony-forming cell (BL-CFC) assays [3] on EB6 cells under HOXB4-off or -on conditions. Unexpectedly, c-Kit$^+$CD41$^+$ cells exhibited scant BL-CFC activity, and c-Kit$^+$CD41$^-$ cells instead were significantly enriched in BL-CFC, regardless of HOXB4 expression status (Fig. 3A). The potentials to give rise to blood cells and vascular endothelial cells in BL-CFC were examined on a clonal basis as previously described [20]. Most of these blast colonies individually exhibited hematopoietic and/or endothelial differentiation potential (Fig. S2). Of note is that neither BL-CFCs nor cells composing blast colonies significantly respond to HOXB4 expression (Fig. 3A and Fig. S2). Consistent with BL-CFC data, most vasculogenic activity was detected in CD41$^-$ cells (Fig. 3B). In contrast, most primitive erythropoietic activity was detected in CD41$^+$ cells (Fig. 3C), as in the yolk sac (YS) [15], supporting the view that primitive hematopoietic progenitors arise soon after the development of mesoderm [21]. Primitive erythroid colony formation was significantly inhibited by HOXB4 expression (Fig 3C).

## Genes expressed in EB6 subpopulations

RT-PCR was performed on cDNAs prepared from fractionated EB6 cells. Consistent with recently published data[14], all genes examined, including *Runx1*, *Scl*, *Gata1*, and *Gata2*, were expressed in c-Kit$^+$CD41$^+$ cells (Fig. S3), suggesting that this population at this developmental stage is already in the process of establishing definitive hematopoiesis. Expression of *Gata1*, *β-H1 globin* (*Hbb-bh1*), and *β-major globin* (*Hbb-b1*), detected in c-Kit$^-$CD41$^+$ and c-Kit$^+$CD41$^+$ cells, supports observations that these two populations contain primitive erythrocyte precursors (EryPs). *Flk1* expression with faint *Brachyury* expression in both c-Kit$^+$CD41$^-$ cells and c-Kit$^+$CD41$^+$ cells implies that these populations are the immediate progeny of mesodermal precursors. Although low levels of endogenous mouse *HoxB4* expression were detected in c-Kit$^+$CD41$^+$ cells, higher expression levels might be required for generation of HSCs.

## Cell surface markers on long-term repopulating cells derived from EB cells

In order to define HSC phenotypes just before transplantation, CD41$^+$ EB6 cells were co-cultured with OP9 cells and were induced

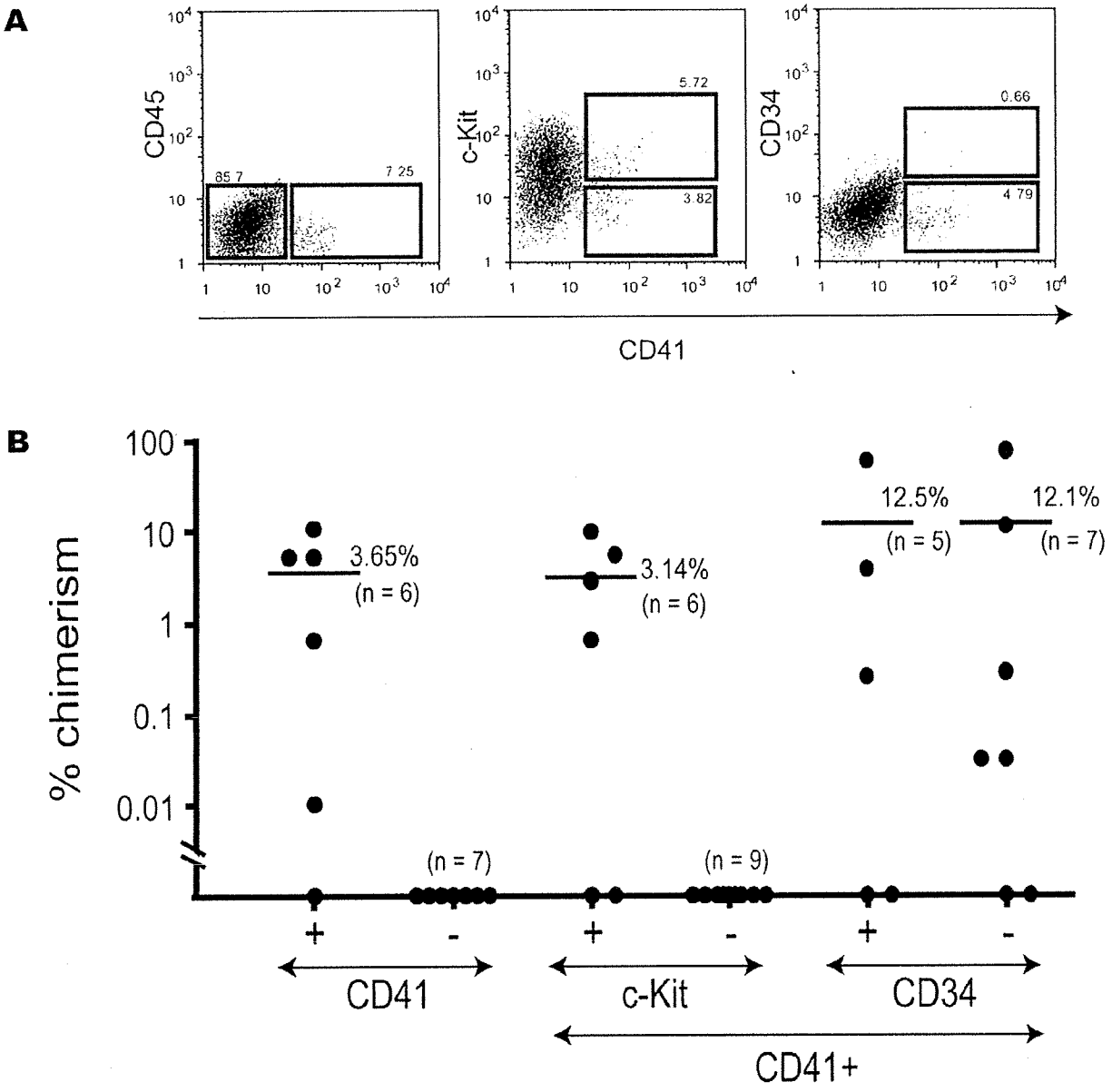


**Figure 2. EB6 subpopulations with the potential of giving rise to HSCs. (A)** Data from flow cytometry analysis show the expression of CD41, CD45, c-Kit, and CD34 in EB6 cells. The sorting gates for $CD41^-$ or $CD41^+$ cells, $c\text{-}Kit^+CD41^+$ or $c\text{-}Kit^-CD41^+$ cells, and $CD34^+$ $CD41^+$ or $CD34^-CD41^+$ cells are indicated as squares. **(B)** EB6 cells were fractionated based on expression of CD41, c-Kit, and CD34, co-cultured with OP9 cells for 4 days, sorted for GFP+ cells, and transplanted into lethally irradiated mice. HOXB4 expression was maintained from *in vitro* co-culture through *in vivo* repopulation. Recipient mice were analyzed 16 weeks after transplantation. Over 95% of reconstituted blood cells were of myeloid lineage in all cases (data not shown). Two independent experiments gave similar results. Data from one experiment are shown. See Table S1 for the number of transplanted cells from each subpopulation.
doi:10.1371/journal.pone.0004820.g002

to express HOXB4. HOXB4-expressing cells, detected as $GFP^+$ cells, were analyzed for expression of cell surface markers. $GFP^+$ cells were fractionated based on expression of CD41, c-Kit, CD34, or CD45 by flow cytometry (Fig. 4A) and were transplanted into lethally irradiated mice with rescue cells (Table S2). Analysis of recipient mice 16 weeks after transplantation showed that $CD41^+$ cells, $c\text{-}Kit^+$ cells, $CD34^+$ cells, and $CD45^-$ cells were enriched in long-term repopulating activity (Fig. 4B). Myeloid lineage was predominantly reconstituted in all cases. Numbers of $CD41^+$, $c\text{-}Kit^+$, and $CD34^+$ cells apparently decreased in the absence of HOXB4 expression (data not shown). These data indicate that HOXB4 expression selectively maintains the $c\text{-}Kit^+CD41^+$ $CD45^-$ phenotype and up-regulates CD34 expression during the co-culture period. It is known that fetal liver HSCs express CD34 antigen while adult bone marrow HSCs barely express CD34 antigen [22,23]. These data suggest that ESC-derived HSCs remain phenotypically immature.

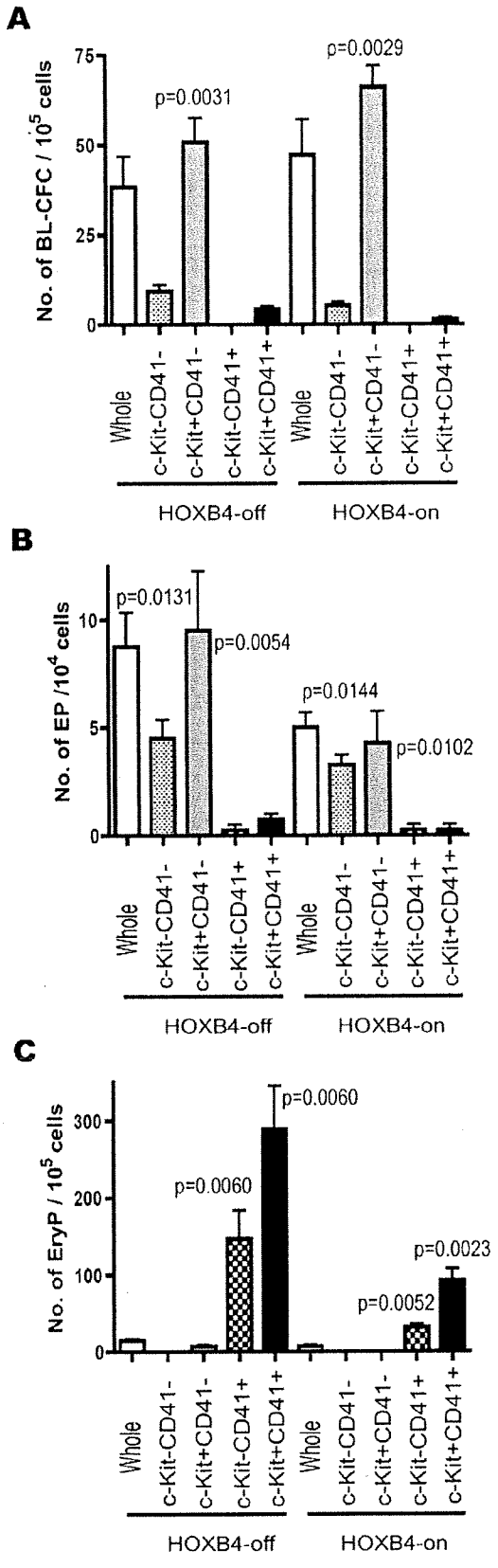


**Figure 3. Hemangioblastic, endothelial, and primitive erythrocytic potentials among EB6 subpopulations.** Colony forming abilities in unfractionated, c-Kit$^-$CD41$^-$, c-Kit$^+$CD41$^-$, c-Kit$^-$CD41$^+$, or c-Kit$^+$CD41$^+$ EB6 cells were examined in quadruplicate. **(A)** Blast colony-forming assays were performed. **(B)** Vascular endothelial progenitors (EP) were detected by the OP9 co-culture system with cytokines as previously described [20]. **(C)** Erythroid colonies were detected by methylcellulose colony assays. Detected erythroid colonies contained primitive erythrocytes as identified by *β-H1 globin* expression (data not shown). Kruskal-Wallis testing was performed for statistical analysis.
doi:10.1371/journal.pone.0004820.g003

## *In vivo* function of HSCs derived *in vitro* from ESCs

We observed that c-Kit$^+$CD41$^+$ cells had accumulated in the bone marrow of recipient mice when analyzed 18 weeks after transplantation (Fig. S4). We attempted to shut HOXB4 expression off in recipient mice from 8 to 14 weeks after transplantation by letting them drink water containing 100 μg/ml of Dox. Analysis of peripheral blood cells from these mice showed that GFP$^+$ cells became undetectable and that B- and T-lymphoid lineage reconstitution was significantly improved. Myeloid lineage reconstitution, contrariwise, was reduced, with decreases in total chimerism (data not shown). After GFP$^+$ bone marrow cells were isolated from other mice reconstituted with ESC-derived cells, $1.2\times10^5$ GFP$^+$ cells together with $2\times10^5$ rescue cells was transplanted into each of 6 lethally irradiated mice, of which 3 were given Dox and 3 were not. Of the 3 recipients given Dox, 2 mice showed 0.8% and 15% chimerism, with respectively 46 : 54% and 50 : 50% myeloid : lymphoid lineages. Of the 3 recipients not given Dox, 4 mice showed 45% and 83% chimerism with almost exclusively myeloid lineage. These results support the hypothesis that HOXB4 expression negatively affects lymphoid differentiation and positively affects repopulating activity in ES-derived HSCs [11], effects not seen in adult HSCs [24].

## HOXB4 target genes in HSC development

Our last experiments compared gene expression profiling among c-Kit$^+$CD41$^+$ EB6 cells (cells with the potential to give rise to HSCs), c-Kit$^+$CD41$^+$ cells after co-culture with HOXB4 expression (repopulating cells), and c-Kit$^+$CD41$^+$ cells after co-culture without HOXB4 expression (non-repopulating cells). We attempted to identify candidate genes whose expression is up- or down-regulated by HOXB4, among which might exist important genes that control the early development of HSCs. To verify the Tet-off strategy, HOXB4 expression was examined in these 3 populations and in ESCs maintained in the presence of Dox (ESCs without HOXB4 expression). As expected, *HOXB4* expression was only detected in c-Kit$^+$CD41$^+$ EB6 cells after co-culture without Dox (Fig. S5).

Microarray analysis was performed on cDNAs prepared from c-Kit$^+$CD41$^+$ EB6 cells without HOXB4 expression and c-Kit$^+$CD41$^+$ cells after co-culture with or without HOXB4 expression. In order to focus on genes up- and down-regulated by HOXB4 expression, we employed stringent criteria (Legends, Tables S3 and S4). Genes with 5-fold or more difference in gene chip scores between c-Kit$^+$CD41$^+$ cells after co-culture with HOXB4 expression and c-Kit$^+$CD41$^+$ cells without HOXB4 expression were selected.

After selection, 294 and 115 probes, respectively, remained for HOXB4 up- and down-regulated genes. We next examined whether these selected genes are expressed in HSCs via gene expression profiling of adult HSCs. HSC-expressing genes shared 200 of 294 probes for HOXB4 up-regulated genes. Of great interest is that *CD34*, *CD150* (*Slamf1*), *c-Mpl*, *integrin α4* and *α6* (*Itga4* and *6*), and *transforming growth factor β type II receptor* (*Tgfbr2*) were among them. On the other hand, 58 of 115 probes for down-regulated genes by HOXB4 were not detected on adult HSC

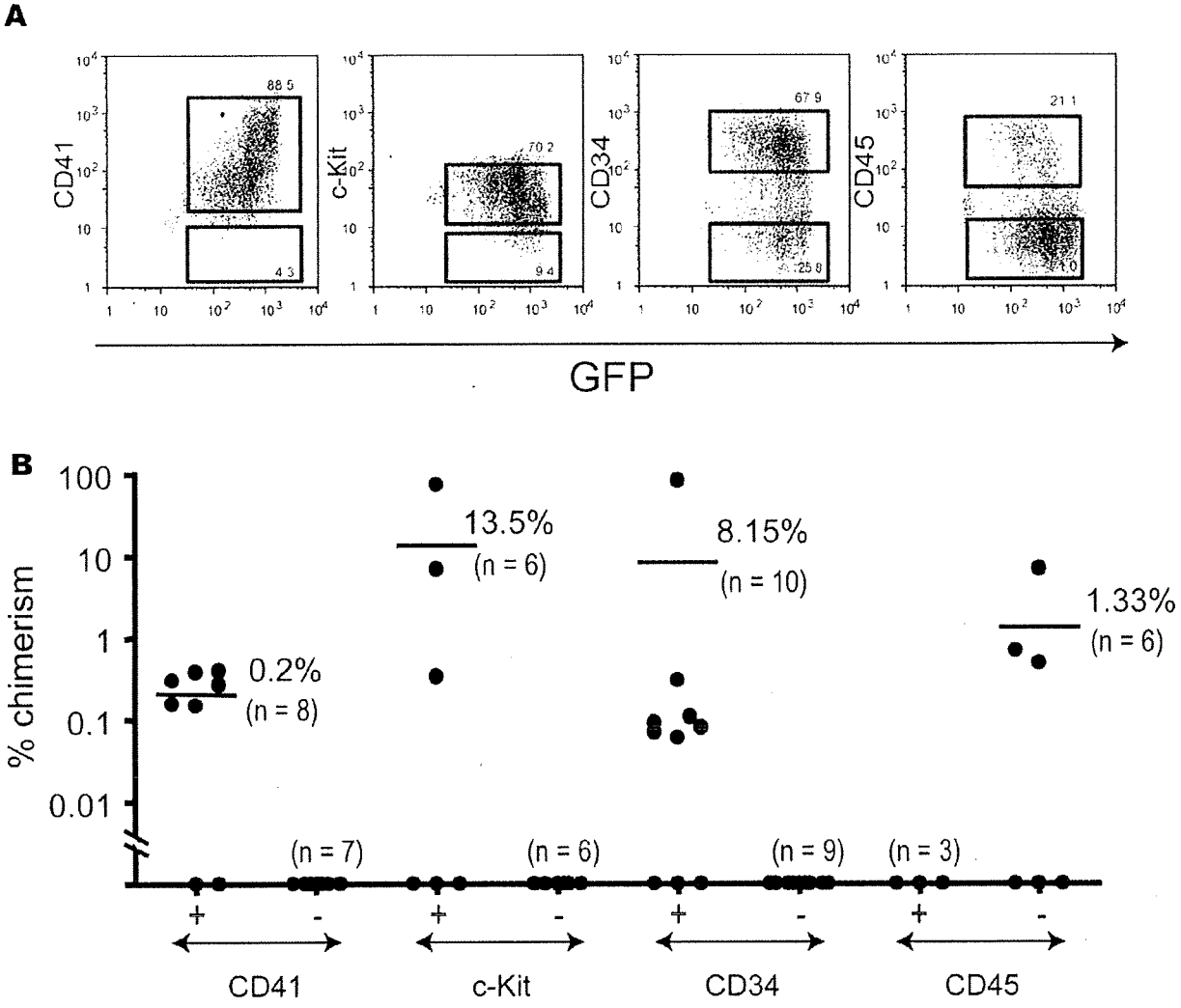


**Figure 4. Surface markers of embryonic HSCs generated from EB6 cells *in vitro*.** **(A)** $CD41^+$ EB6 cells were co-cultured with OP9 cells in the absence of Dox for 4 days. Cells collected from the co-cultures were analyzed by flow cytometry. HOXB4-expressing cells were detected by GFP expression. Data show the expression of CD41, c-Kit, CD34, and CD45 in $GFP^+$ cells. The sorting gates for $CD41^-$ or $CD41^+$ cells, c-$Kit^-$ or c-$Kit^+$ cells, $CD34^-$ or $CD34^+$ cells, and $CD45^-$ or $CD45^+$ cells are shown as squares. **(B)** Co-cultured cells were fractionated based on expression of CD41, c-Kit, CD34, and CD45, and were transplanted into lethally irradiated mice. Recipient mice were analyzed 16 weeks after transplantation. Over 95% of reconstituted blood cells were of myeloid lineage in all cases (data not shown). Two independent experiments gave similar results. Data from one experiment are shown. See Table S2 for the number of transplanted cells for each subpopulation.
doi:10.1371/journal.pone.0004820.g004

profiling. All up-regulated adult HSC-related genes and all down-regulated adult HSC-unrelated genes are listed in Tables S3 and S4 and are also schematically presented as a heat map in Fig. 5A. The overall similarity in the heat map between the EB6 and the HOXB4-off samples suggests that these data represent the effect of enforced expression of HOXB4. RT-PCR analysis showed that the expression levels of *CD150* and *c-Mpl* were significantly higher in HOXB4-on c-$Kit^+CD41^+$ cells than in HOXB4-off c-$Kit^+CD41^+$ cells, and that the expression levels of *βh1-globin* (*Hbb-bh1*) and *Lin28* were significantly lower in HOXB4-on c-$Kit^+CD41^+$ cells than in HOXB4-off c-$Kit^+CD41^+$ cells (Fig. 5B). A marked increase in $CD34^+$ repopulating cells (Fig. 4) and a marked decrease in primitive erythroid progenitors (Fig. 3) with HOXB4 expression were consistent with the gene expression profiling data.

A number of genes are implicated as playing important roles in the generation of HSCs. According to our microarray data, significant levels of Scl, Runx1, Gata2, or Lmo2, were expressed in c-$Kit^+CD41^+$ cells, but induced HOXB4 expression did not change their expression levels. Expression levels of Cdx1 and Cdx4 remained low in c-$Kit^+CD41^+$ cells regardless of HOXB4 expression.

## Discussion

This study demonstrates that pre-HSCs, perhaps conceptually relevant to hemogenic endothelium [25], can be prospectively isolated from developing mouse EBs. Pre-HSCs were unable to engraft and to reconstitute the hematopoietic system in lethally

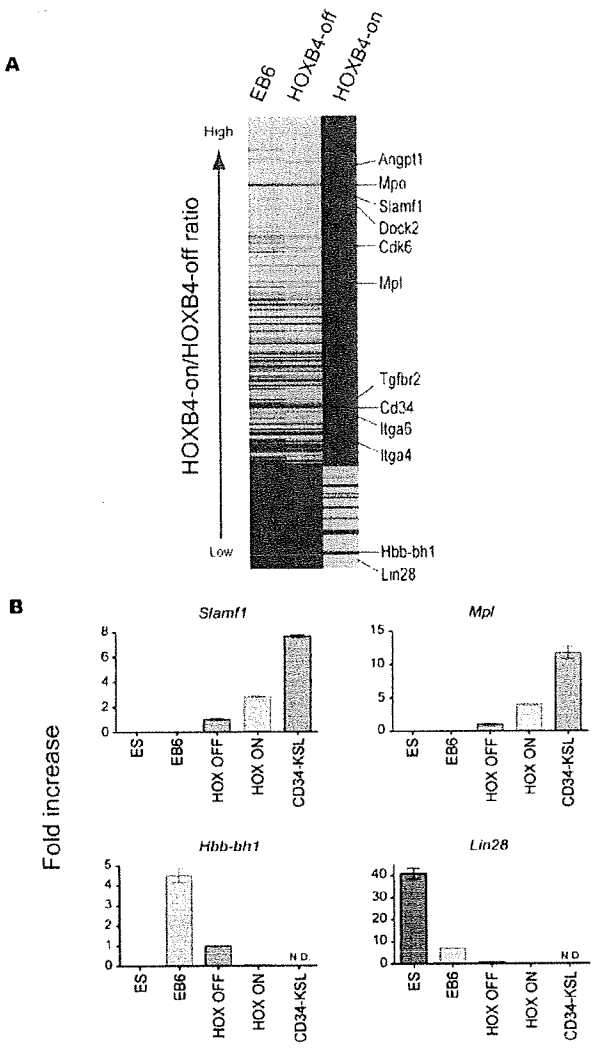


**Figure 5. Heat map of differentially expressed genes. (A)** Microarray analysis was performed on cDNAs from c-Kit$^+$CD41$^+$ EB6 cells without HOXB4 expression, c-Kit$^+$CD41$^+$ cells after co-culture without HOXB4 expression, and c-Kit$^+$CD41$^+$ cells after co-culture with HOXB4 expression. The finally selected 223 genes are shown in this graph (for selection criteria, see Legend, Table S3). Red indicates genes up-regulated 5-fold or more. Blue indicates genes down-regulated 5-fold or more. **(B)** Real-time PCR was performed on normalized cDNA from the cells described above, from ESCs maintained without HOXB4 expression, and from CD34$^-$KSL cells from adult bone marrow. The mean plus or minus 1SD (n = 3) is shown for 4 representative genes.
doi:10.1371/journal.pone.0004820.g005

irradiated adult mice. To engraft in adult mice, pre-HSCs should acquire both engraftment and repopulating capacities. This developmental process was driven or enhanced by enforced expression of HOXB4. Contrary to previous studies [11], HOXB4 had to be continuously expressed *in vivo* after transplantation to maintain long-term repopulation in this study. When HOXB4 expression was turned off in some reconstituted mice, myeloid reconstitution level was decreased while B- and T-lymphoid reconstitution levels were increased. As a result, the total chimerism was gradually reduced (data not shown). We used a Tet-off system while Kyba et al. used a Tet-on system. An explanation for this discrepancy may be that Tet-on systems are "leaky" by comparison with Tet-off systems, permitting weak persistent expression of HOXB4 even after turn-off in the work of Kyba *et al.* Long-term repopulating cells generated from pre-HSCs by OP9 co-culture and HOXB4 expression persistently showed low levels of long-term reconstitution. When $10^5$ adult bone marrow cells, instead of Sca-1$^-$ rescue cells, were used as competitor cells, reconstitution became undetectable (data not shown). A similar property has been observed for HSCs from the YS and P-Sp/AGM region. We operationally called these HSCs with low repopulating potential embryonic HSCs.

As previously noticed [11], HOXB4 overexpression seemed to have prevented lymphoid reconstitution, with long-term reconstitution mainly myeloid in this study. Multilineage reconstitution has been a criterion for HSCs. However, myeloid reconstitution may be more reliable than lymphoid reconstitution as a marker of HSC activity because short-lived granulocytes are never detectable in the circulation for long unless they are continuously supplied by engrafted HSCs.

Pre-HSCs and embryonic HSCs are distinct populations in function and gene expression profiling, but they both exhibited the c-Kit$^+$CD41$^+$CD45$^-$ phenotype. Since c-Kit is already expressed in a significant proportion of undifferentiated ESCs and in most YS, P-Sp/AGM, fetal liver, and adult bone marrow HSCs [6,26,27,28], the maintenance of this receptor tyrosine kinase may be crucial for the development of HSCs from the internal cell mass.

CD41 marks both primitive and definitive hematopoiesis [15,16,17,18]. The developmental wave of definitive but transient hematopoiesis clearly differs from that of HSCs [1,2]. Whether CD41 also marks HSCs in their early development has been uncertain. In this study, pre-HSCs and primitive erythroid progenitors were detected among CD41$^+$ cells (Figs. 2B, 3C). In contrast, hemangioblastic and vasculogenic activities were principally detected in CD41$^-$ cells.

Hemangioblasts are thought to play a major role in initiation of primitive and definitive hematopoiesis [3]. HSCs have been generally believed to arise from hemangioblasts [7]. Unlike previous studies[3], our blast colony assays were performed on EB6 cells instead of EB3.0 or 3.5 cells. This might be the reason that pre-HSC and hemangioblast activities were detected in the separated populations. Pre-HSCs may develop closely associated with hemangioblasts because these two types of cells arise from common mesodermal precursors at a very early point. It is important to clarify at which stage these cell classes separate from one another during development. Our data suggest that pre-HSCs are separated from hemangioblasts as soon as they arise. The possibility exists that pre-HSCs initially develop through hemangioblasts, but soon thereafter these two types of cells become distinct from one another. Alternatively, HSCs develop independent of hemangioblasts. Since *in vitro* differentiation of ESCs along the blood lineage mostly mimics YS hematopoiesis [29], it is possible that pre-HSCs arise in close association with YS development. In this case, pre-HSCs presumably are unable efficiently to differentiate into embryonic HSCs in the YS microenvironment, but, after migration, are able to do so in particular developmental niches like the P-Sp/AGM region [4,5] and the fetal liver microenvironment.

Although fetal and adult HSCs express CD45, pre-HSCs and embryonic HSCs were shown not to express CD45. Most HSCs from the YS and P-Sp/AGM region at E10.5 or earlier do not express CD45 [19,30]. In this regard, CD45 is a late maturation marker of HSCs whereas CD41 is an early maturation marker of HSCs. Identification and characterization of c-Kit$^+$CD41$^+$CD45$^-$ pre-HSCs and embryonic HSCs in early developing embryos will clarify the significance of changes in HSC phenotype.

We and others have been interested in target genes of HOXB4. If other HSC inducers are indentified among such molecules, more efficient generation of HSCs should become possible. A large number of candidate target genes has been reported recently [31]. Unfortunately, these expressed genes were not always identified among populations properly enriched in HSC activity. We therefore used c-Kit$^+$CD41$^+$ cells from which HSC activity emerged after HOXB4 expression was turned on.

Among a number of candidate genes obtained in this study were many genes known to be expressed in adult HSCs (Table S3). Of special note is that *CD34*, *CD150*, and *c-Mpl* are up-regulated in the transition of pre-HSCs to embryonic HSCs. Only some pre-HSCs expressed CD34, but all embryonic HSCs derived from pre-HSCs expressed CD34 (Fig. 4). That CD34 is expressed in YS and P-Sp/AGM HSCs [6,32] supports the inference that all these cells are closely related. CD150, which is expressed from fetal HSCs to adult HSCs, is a new HSC marker [33,34]. c-Mpl, the receptor for TPO, is expressed in most fetal and adult HSCs. Although the function of CD34, CD150, or c-Mpl is not essential for the development of HSCs [12,35,36], it is suggested that these HSC markers begin to be expressed at the embryonic HSC stage. CD34, CD150, and c-Mpl could be good candidates for the earliest markers during HSC development. Since many intracellular molecules (*e.g.*, angiopoietin 1 and myeloperoxidase) were also up-regulated, they might also serve as markers for embryonic HSCs. Angiopoietin 1, secreted by HSCs in the P-Sp/AGM region, fetal liver, and adult bone marrow, has been suggested to promote angiogenesis [37]. High levels of expression of these molecules might be tightly associated with commitment to HSC lineage. The origin of HSCs – YS or P-Sp/AGM region – has been debated for a very long time. It is difficult to determine precisely which site is the first origin of HSCs because in the mouse embryo the P-Sp/AGM region does not exist at E7, when the YS begins to appear. A combination of markers listed in this study should be useful for *in vivo* detection of embryonic HSCs.

Fetal and adult HSCs are functionally distinct [38,39]. Pre-HSCs and embryonic HSCs are functionally different from fetal and adult HSCs. Our working model for HSC development is presented in Fig. 6. We propose that pre-HSCs which arise from mesoderm, possibly independent of hemangioblasts, give rise to embryonic HSCs which subsequently give rise to fetal and adult HSCs. Whether all adult HSCs are generated by fetal HSCs remains uncertain, as recently suggested [40]. These processes should take place in spatially and temporally established niches in developing embryos. Certainly much more work is required, but identification and characterization of pre-HSCs and embryonic HSCs in developing embryos are central to validation of this model.

Embryonic stem cells (ESCs) hold great promise to innovate a variety of new therapies for regenerative medicine because of their potential of differentiating into all sorts of adult cells. The key to success in stem cell therapy is to establish methods of properly differentiating ESCs into any particular type of tissue-specific stem cells. Recent establishment of induced pluripotent stem cell lines [41,42] demands more such protocols. In order to generate HSCs from ESCs efficiently *in vitro*, optimal conditions must be determined for each developmental step in our model.

## Materials and Methods

### Mice

129/OlaHsd (129Ola) mice were purchased from Jackson Laboratory (Bar Harbor, ME). Ly5 congenic C57BL/6 mice (B6-Ly5.1) were obtained from Sankyo Laboratory Service (Tsukuba, Japan). 129Ola and B6-Ly5.1 mice were mated to produce F1 mice (Ly5.1×Ly5.2). Mice were maintained in the Institute of Medical Science University of Tokyo Animal Research Center. All experiments using mice received approval from the Institute of Medical Science Animal Experiment Committee.

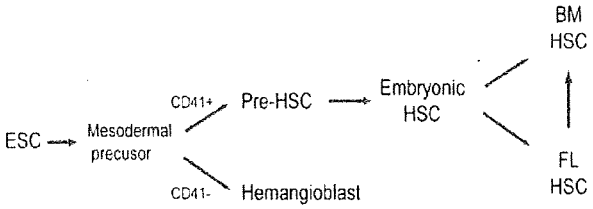


**Figure 6. A stepwise developmental model for HSCs.** We propose a working model for HSC development. Pre-HSCs originate from mesoderm, possibly independent of hemangioblasts; pre-HSC give rise to embryonic HSCs in particular niches in the YS or P-Sp/AGM region; embryonic HSCs give rise to fetal and adult HSCs in particular niches in the fetal liver and bone marrow.
doi:10.1371/journal.pone.0004820.g006

### ESCs

The mouse ES cell line EB3, derived from E14tg2a ESCs, was maintained without mouse embryonic fibroblasts in Glasgow minimum essential medium supplemented with 10% fetal calf serum (FCS) (JRH Bioscience, Lenexa, KS), 0.1 mM 2-mercaptoethanol (2-ME), 2 mM L-glutamine (L-Gln), 0.1 mM non-essential amino acids, 1 mM sodium pyruvate (Invitrogen, Carlsbad, CA), 1,000 U/ml leukemia inhibitory factor (LIF, Chemicon, Temecula, CA), and 100 U/ml penicillin/streptomycin. For these cultures, a 100 mm-tissue culture dish was used after coating with 5 ml of 0.1% gelatin in PBS for 10 min at 37°C.

### Tet-regulated HOXB4/GFP expression in ESCs

The tetracycline (Tet)-off system was chosen because gene expression is more strictly controllable in the Tet-off system than in the Tet-on system [43]. ESCs carrying the Tet-off iHOXB4 expression cassette in the ROSA26 locus (iHOXB4 ESCs) were made as previously described (Fig. S6) [44].

### *In vitro* ESC differentiation

iHOXB4 ESCs were maintained in the presence of 1 μg/ml doxycycline (Dox), a tetracycline derivative. To allow ESCs to differentiate into EBs, ESCs were trypsinized and collected in complete EB differentiation medium (EBD) [3]. Cells were transferred into a 100-mm Petri dish at $2\times10^5$ cells per 10 ml EBD. The medium was changed on day 4 of culture and every 2 days thereafter.

### Co-culture with OP9 cells

OP9 cells were maintained in α-MEM containing 15% FCS. $10^5$ OP9 cells were plated in each well of a 6-well tissue culture plate 2 days before starting co-culture. Developed EBs were treated with 0.25% trypsin for 4 min at 37°C and were disrupted to yield single cells. Co-cultures were employed with IMDM containing 20 ng/ml mouse stem cell factor (SCF) and 20 ng/ml human thrombopoietin (TPO), 10% FCS, 2 mM L-Gln, 0.1 mM 2-ME, and 100 U/ml penicillin/streptomycin. On specified days of co-culture, cells were recovered from the culture dishes for analysis and sorting on a flow cytometer.

### Flow cytometry analysis and sorting

ESCs, EB cells, and cells after OP9 co-culture were stained with phycoerythrin-conjugated (PE-) anti-Flk-1 (eBioscience, San

Diego, CA), allophycocyanin-conjugated (APC-) anti-CD31, biotinylated anti-CD34, PE-anti-CD41, and APC-anti-c-Kit antibodies (BD Biosciences, San Jose, CA) on ice for 30 min. Streptavidin-APC-Cy7 (BD Biosciences) was used for detection of biotinylated antibody. Analysis and sorting were performed on a MoFlo (DAKO, Glostrup, Denmark).

### Methylcellulose colony assays

Cells were cultured in 1% methylcellulose containing 30% FCS, 1% bovine serum albumin, 2 mM L-glutamine, and 0.05 mM 2-ME. For colony assays, 10 ng/ml mouse interleukin-3, 10 ng/ml SCF, 2 U/ml human erythropoietin, and 50 ng/ml TPO were included. Cells were incubated at 37°C in a humidified atmosphere with 5% $CO_2$ in air. Colonies were counted on day 10 of culture and individually picked up. Each colony was cytocentrifuged onto a glass slide for morphological examination with May-Gruenwald-Giemsa staining. Primitive erythroid colonies were counted on day 3 of culture. Blast colony assays were performed as previously described [16]. In brief, cells were cultured in IMDM containing 1% methylcellulose, 10% FCS, $4.5\times10^{-4}$ M monothiolglycerol, 1% L-Gln, 25 μg/ml ascorbic acid, 300 μg/ml human saturated transferrin, 5 ng/ml vascular endothelial growth factor, 100 ng/ml SCF, and 5 ng/ml IL-6. Blast colonies were counted on day 4 of culture.

### Long-term reconstitution assays

2- to 3-month-old B6-Ly5.1×129Ola F1 mice (Ly5.1/Ly5.2) were irradiated at a dose of 900 cGy. ES-derived cells (Ly5.2) were transplanted into these mice (Ly5.1/ly5.2) along with $3\times10^5$ Sca-1-depleted (Sca-1$^-$) bone marrow cells from B6-Ly5.1×129Ola F1 mice as rescue cells. To prepare Sca-1$^-$ cells, mononucleated cells were obtained by density gradient centrifugation using Ficoll-Paque PLUS (Amersham Biosciences, Uppsala, Sweden). Cells were stained with anti-Sca-1 antibody-conjugated magnetic beads (Miltenyi Biotec, Bergisch Gladbach, Germany). Sca-1$^+$ cells were magnetically depleted using an LD column (Miltenyi Biotec).

Peripheral blood cells from recipient mice were analyzed 4 and 16 weeks after transplantation. After red blood cell lysis, cells were stained with biotinylated anti-CD45.1 antibody. After washing, cells were stained with PE-anti-CD4, PE-anti-CD8, APC-anti-Gr-1, APC-anti-Mac-1, and PE-Cy7-anti-B220 antibodies and with APC-Cy7-streptavidin. At least $10^5$ cells were analyzed, and data were collected on a FACS Aria (BD Biosciences). Test donor cells' contribution was detected with the GFP marker. Percentage chimerism was defined as percentage of GFP$^+$ cells in peripheral leukocytes. Test donor cells were considered to have contained long-term repopulating cells when chimerism was over 0.01%.

### RT-PCR

PCR was performed on cDNAs from sorted cells as previously described [45]. Primers are listed in Table S5. The PCR program consisted of 38 cycles of 15 sec at 95°C, 15 sec at 56°C, and 20 sec at 72°C.

### Real-time PCR

The PCR primers were designed using a program provided by Roche (https://www.roche-applied-science.com/sis/rtpcr/upl/index.jsp). PCR contained normalized cDNAs, Universal Probe Library Set, and FastStart Universal Probe Master (Roche, Basel, Switzerland). Quantitative PCR analyses were performed in real-time using an ABI PRISM 7900HT (Applied Biosystems, Foster City, CA). The PCR program consisted of 43 cycles of 15 sec at 95°C and 60 sec at 60°C. Each value was divided by the mean value from HOXB4-off samples to be expressed as fold increase.

### Microarray analysis

Total RNA was extracted from 3 sets of cells. The first was c-Kit$^+$CD41$^+$ EB6 cells derived from iHOXB4 ESCs without HOXB4 expression. The second and third were c-Kit$^+$CD41$^+$ cells after co-culture with OP9 cells for 4 days with or without HOXB4 expression. To prepare cells in the last 2 groups, c-Kit$^+$CD41$^+$ EB6 cells were plated onto a monolayer of OP9 cells and were cultured either in the presence or absence of Dox for 4 days. c-Kit$^+$CD41$^+$ cells were again separated from the co-cultures by flow cytometry. To compare gene expression profiles with those of adult HSCs, CD34$^-$c-Kit$^+$Sca-1$^+$Lineage marker$^-$ (CD34$^-$KSL) cells were isolated from C57BL/6 mice as previously described [26]. In order to analyze cycling adult HSCs, CD34$^-$KSL cells were incubated with 50 ng/ml SCF and 50 ng/ml TPO for 24 hours [46]. Integrity of RNA was assessed qualitatively on an Agilent 2100 Bioanalyzer (Agilent Technologies, Santa Clara, CA). cDNA was synthesized with a MessageAmp aRNA Kit (Applied Biosystems). *In vitro* transcription and labeling were performed using One-Cycle Target Labeling and Control Reagents (Affymetrix, Santa Clara, CA) for ESCs and ESC-derived cells, and using Tow-Cycle Target Labeling and Control Reagents (Affymetrix) for adult HSCs. The heat-fragmented probes were hybridized to a Mouse Genome 430 2.0 GeneChip (Affymetrix). The arrays were scanned and analyzed with the Affymetrix GeneChip System. The relative abundance of each gene was estimated from the average difference of intensities.

### Statistical analysis

Mann-Whitney testing was performed when two groups were compared. Kruskal-Wallis testing was performed when multiple groups were compared.

## Supporting Information

**Table S1**
Found at: doi:10.1371/journal.pone.0004820.s001 (0.02 MB PDF)

**Table S2**
Found at: doi:10.1371/journal.pone.0004820.s002 (0.02 MB PDF)

**Table S3**
Found at: doi:10.1371/journal.pone.0004820.s003 (0.18 MB PDF)

**Table S4**
Found at: doi:10.1371/journal.pone.0004820.s004 (0.06 MB PDF)

**Table S5**
Found at: doi:10.1371/journal.pone.0004820.s005 (0.03 MB PDF)

**Figure S1** Effect of HOXB4 expression in generation of CFU-nmEM and surface marker expression. (A) Data show colony formation by 1,000 cells derived from EB. 1,000 cells were obtained from EBs on days 0, 2, 4, 5, 6, and 7 of culture and co-cultured with OP9 cells for 4 days. Cells collected from the co-cultures were plated in methylcellulose. HOXB4 expression was turned off in both OP9 co-cultures and methylcellulose cultures (HOXB4-off), turned on in both (HOXB4-on), or turned on only in OP9 co-cultures (HOXB4-on to -off). The number of colonies was counted and cells composing each colony were morphologically examined. The graphs show the numbers of neutrophil/macrophage/erythroblasts/megakaryocyte (nmEM) colonies extracted from various colonies formed. Continuous expression of HOXB4 in methylcellulose culture was not necessary for nmEM colony formation. The number of colonies is the mean from 2 independent experiments. (B) Cell surface markers were examined during EB formation without HOXB4 expression. Flk-1+ cells were first detected on day 3 of culture; the proportion of Flk-1+ cells markedly increased on the following day and decreased